QUANTIFICATION OF GEOSYNTHETIC BEHAVIOR

J.P. Giroud
GeoSyntec Consultants
Boca Raton, Florida, USA

ABSTRACT: This paper presents state-of-the-art examples to show that, in a wide variety of cases, the behavior of geosynthetics can be quantified using theoretical analyses. Seven examples are reviewed: geotextile filter retention, geotextile filter clogging, geomembrane stress-strain behavior, geomembrane strain concentrations, geomembrane stress cracking pattern, geomembrane wrinkles, and geosynthetic resistance to differential settlement. The selected examples are such that the important behavioral aspect is not the behavior of the structure in which the geosynthetic is incorporated, but the behavior of the geosynthetic itself. In each case, the phenomenon or problem is described, the theoretical analysis is presented, and the results are discussed. Note: This is only a preliminary version of the final paper which will appear in the post-conference proceedings volume.

1 INTRODUCTION

Geosynthetics have pervaded geotechnical engineering to the point where it is no longer possible to practice geotechnical engineering without geosynthetics. The variety of applications where geosynthetics are used, the variety of functions performed by the geosynthetics in these applications, and the variety of geosynthetics lead to a variety of behaviors. In many applications, geosynthetics are part of a geotechnical structure, such as an embankment, and the geosynthetic behavior is intimately linked to the structure behavior. Such geosynthetic behavior may be called "interactive behavior". The geosynthetic follows, to some extent, the movements of the structure, and, as its tension increases, it becomes able to modify, to some extent, the behavior of the structure. This interactive behavior includes interaction at the level of the geosynthetic-soil interface, generally in the form of interface shear strength.

In applications where geosynthetics perform the function of reinforcement, their behavior is typically interactive. The design methods for such applications are adapted from design methods used in geotechnical engineering. Applications where geosynthetics perform the reinforcement function have led to some of the most spectacular structures, some of the most sophisticated research, and some of the most remarkable publications. However, it may be argued that, if geosynthetics were only performing the reinforcement function, their importance in the field of geotechnical engineering would not be what it is today, and there would be no International Geosynthetics Society just like there is no International Geosteel Society. If geosynthetics were only used in applications where their behavior is interactive, geosynthetics would merely be one more tool available to geotechnical engineers to solve their problems. In fact, geosynthetics are not only convenient products but they constitute the basis for a recognized discipline, because they perform a variety of functions, and because in many cases their behavior is not primarily governed by interaction with the behavior of the structure, but is essentially inherent to the geosynthetic. Such geosynthetic behavior may be called "inherent behavior". A typical example of inherent behavior is the wrinkling of a geomembrane exposed to temperature variations: the formation of wrinkles is essentially governed by the physical and mechanical characteristics of the geomembrane.

Certainly, the behavior of a geosynthetic is neither completely interactive nor completely inherent. For example, the formation of geomembrane wrinkles depends on the interface friction between the geomembrane and the underlying soil. However, there are clearly cases where the design or the observed phenomenon are more influenced by the inherent characteristics of the geosynthetic than by the behavior of the considered geotechnical structure.

The purpose of this paper is to present a few cases of inherent behavior of geosynthetics, and to show that such behavior can be quantified as well as is quantified the interactive behavior. However, whereas the quantification of geosynthetic interactive behavior (in applications such as reinforced embankments) can be achieved using methods adapted from those used in conventional geotechnical engineering, the quantification of geosynthetic inherent behavior requires the development of original methods.

The following examples will be used to illustrate the inherent behavior of geosynthetics:

- geotextile filter retention;
- geotextile filter clogging;
- geomembrane stress-strain behavior;
- geomembrane strain concentrations;
- geomembrane stress cracking pattern;
- geomembrane wrinkles; and
- geosynthetic resistance to differential settlement.

In each case, a theoretical analysis will be presented briefly (with references to other publications for more details) and the findings of the analysis will be discussed thoroughly. Discussions will include philosophical aspects, such as comments on the power of rational analysis, and practical aspects, such as recommendations to design engineers.

2 GEOTEXTILE FILTER RETENTION

2.1 Overview

A filter used in geotechnical engineering must have openings small enough to retain the soil and, at the same time, must be permeable enough to allow water to pass as freely as possible. In other words, the filter must meet a retention criterion and a permeability criterion. These two criteria are, to some extent, contradictory because the permeability of a filter increases with increasing opening size. However, in the majority of cases, it is possible to find a filter material, sand or geotextile, that has openings small enough to retain the soil and, at the same time, large enough to ensure that the filter permeability is sufficiently high for the considered case. In other words, it is generally possible to find a filter that meets both the retention criterion and the permeability criterion. In this section, it is assumed that the permeability criterion is met by the filter, and only the retention criterion is discussed.

Common sense dictates that, to retain the soil, the filter must prevent the migration of soil particles and, therefore, the largest opening of the filter must be smaller than the smallest soil particle. However, common sense, as is often the case, is wrong. Soil retention does not require that the migration of all soil particles be prevented. Soil retention simply requires that the soil behind the filter remain stable; in other words, some small particles may migrate into and/or through the filter provided that this migration does not affect the soil structure, i.e., does not cause any movement of the soil mass. (Of course, the filter and the drainage medium located downstream of the filter should be such that they can accommodate the migrating particles without significant clogging. This important point will be addressed in Section 3; only retention is discussed herein.) It should be noted that the "smallest" soil particle is potentially so small that the common sense requirement mentioned above would lead to selecting a quasi-impermeable membrane as a filter, which is absurd because it could not meet the permeability criterion. The common sense requirement that openings should be smaller than the smallest particles only applies to sieving, where particles are constantly agitated, until they pass if they can.

The above discussion is not unknown to geotechnical engineers. They are accustomed to designing sand filters or selecting the openings of perforated draining pipes using not the size of the "smallest" soil particle, but the size of a particle that is almost the largest soil particle: they use d_{85} , the size of the soil particle that is such that 85% by weight of the soil particles are smaller than d_{85} . (d_{85} is used and not d_{100} , the size of the largest soil particle, because the measurement of d_{100} is likely to fluctuate significantly from one sample to another if there are only a few large particles which may be present in one sample and not in another, whereas the value of d_{85} is less likely to fluctuate due to the large number of soil particles that have the d_{85} size in a typical soil sample.) Clearly, the traditional approach in geotechnical engineering is to consider that, if the quasi-coarsest soil particles (defined by d_{85}) are retained, the entire soil is retained. The assumed mechanism is that the coarsest soil particles form a matrix that entraps other soil particles and prevents them from moving. The soil structure is stable if this mechanism works at every particle size level. In other words, particles of any given size must be entrapped in the matrix formed by particles of a larger size. Therefore, it is implicitly assumed that the soil contains a fair share of particles of each size, in other words that the particle size distribution of the soil is continuous ("well-graded" soils). In the case of a gap-graded soil that contains a large proportion of coarse particles and a proportion of fine particles too small to fill the voids between coarse particles, it is clear that the fine particles can migrate between the coarse ones and, therefore, are not entrapped. Gap graded soils are not considered in this discussion.

Assuming that the soil particle size distribution is continuous ("well-graded" soil), is it correct to consider, as geotechnical engineers may tend to do, that geotextile filters should be designed by simply writing that the geotextile maximum opening size should be smaller than the soil d_{85}? If this were correct, the retention criterion would be very simple:

$$O_{95} < d_{85} \qquad (1)$$

where: O_{95} = geotextile apparent opening size (AOS). (It should be noted that O_{95} is traditionally used instead of O_{100} , just as d_{85} is used instead of d_{100} , for reasons of reliability of measurement, as discussed above.)

The analysis presented below shows that, in some cases, values of the filter opening size significantly larger than given by the above equation may be used, whereas in other cases it is dangerous to use the above equation and values of O_{95} significantly lower than d_{85} should be used.

2.2 Summary of Theoretical Analysis

As indicated above, a geotechnical filter can only work if the retained soil is internally stable. Internal stability of a soil depends on many parameters. A soil can be internally stable if there is sufficient cohesion between its particles. Cohesive soils are not discussed herein, only cohesionless soils are considered. Also, any soil, even very stable, may be disorganized by large external forces especially repeated forces such as those resulting from wave action. Only filters subjected to steady flow in porous media are considered herein, such as filters used in drainage systems.

The problem with Equation 1, derived from geotechnical engineering practice, is that it implicitly assumes, as mentioned above, that the soil is internally stable provided its particle size distribution curve is continuous. This is not necessarily the case. Continuity of the particle size distribution curve is a necessary, but not sufficient, condition to ensure the internal stability of a cohesionless soil. For a cohesionless soil to be internally stable, particles of any given size must be entrapped in the matrix formed by particles of a larger size. As indicated by Giroud (1982), this is only possible if the particle size distribution of the soil has a coefficient of uniformity of 3 or less ($C_u \leq 3$) (Figures 1a and 2).

If a soil has a coefficient of uniformity greater than 3 (Figure 1b and 2), there are not enough of the largest particles to form a matrix where smaller particles are interlocked. It is only at a lower level of particle size that exists a matrix of particles where smaller particles are interlocked.

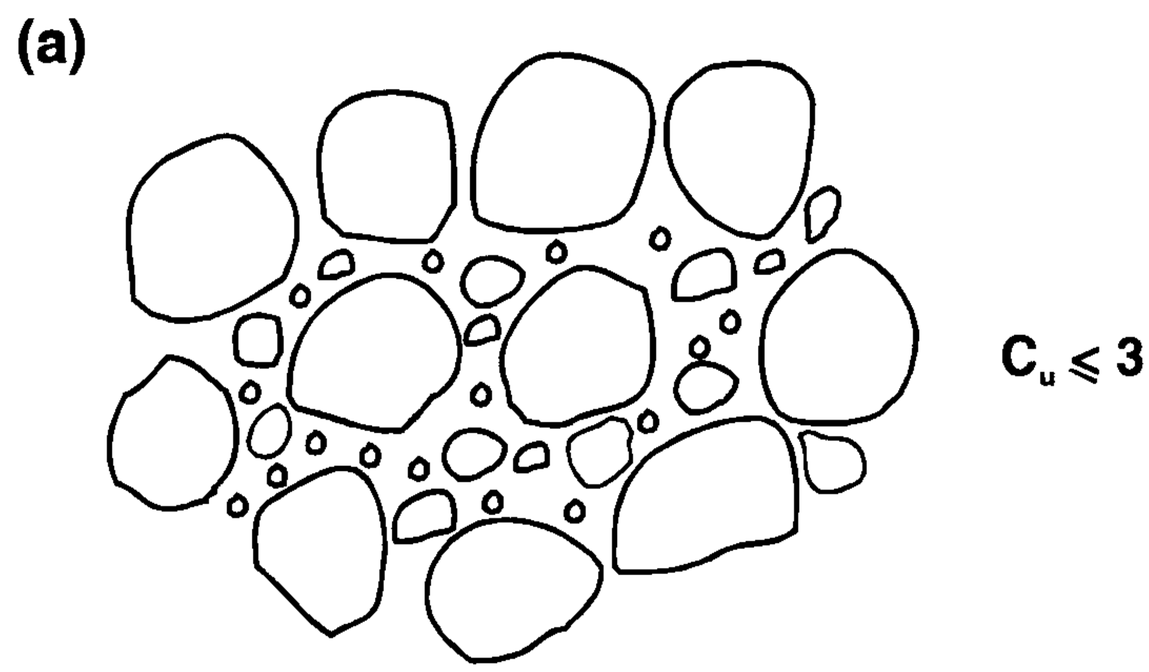

Fig. 1 Schematic representation of particle size distributions.

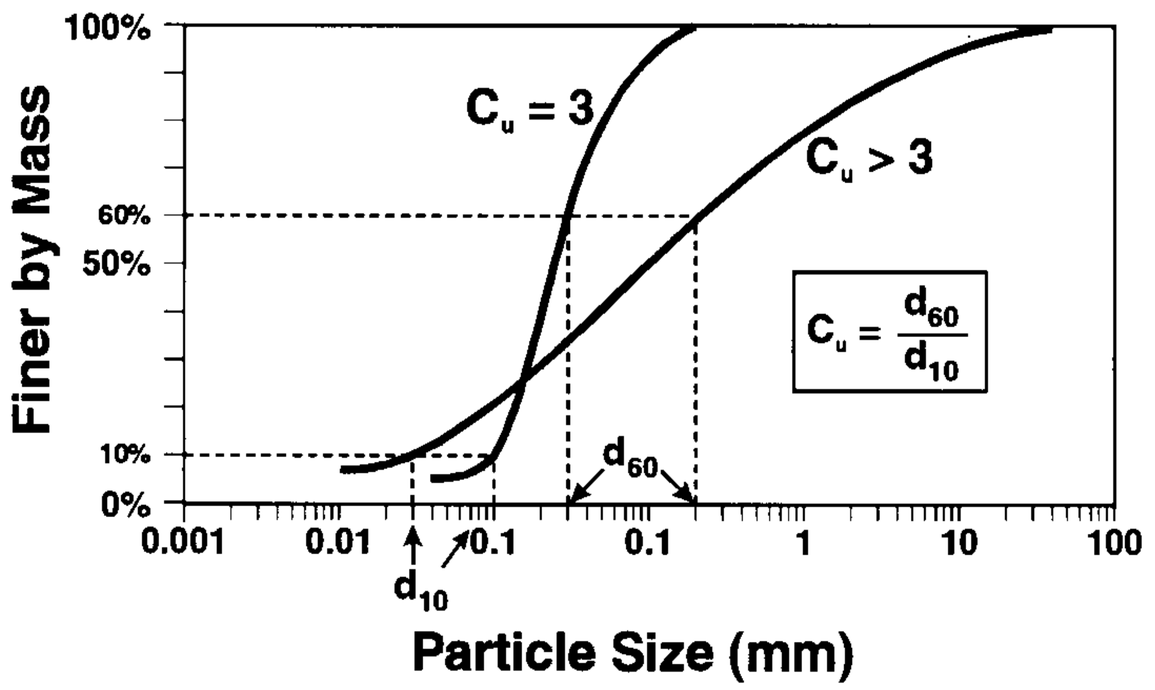

Fig. 2 Soil particle size distribution.

If the coefficient of uniformity of the soil is 3 or less ($C_u \leq 3$), a geotextile filter that just retains the largest soil particles is adequate: it retains all the soil because all soil particles are entrapped in the matrix formed by the largest soil particles. If the coefficient of uniformity of the soil is greater than 3, a geotextile filter that just retains the largest soil particles does not retain all the soil: in this case, smaller particles are not entrapped within a matrix formed by the largest particles and they pass through the geotextile filter if they are dragged by flowing water. Clearly, if the coefficient of uniformity

of the soil is greater than 3, the geotextile filter must be designed to retain not the largest soil particles, but the particles that form a matrix where the smaller particles are entrapped. In other words, if the coefficient of uniformity of the soil is greater than 3, the design of the filter should ignore the largest particles and only consider the particles that, if they were alone, would form an internally stable soil, i.e., a soil with a coefficient of uniformity of 3. As shown in Figure 3, this leads to selecting a filter that just retains soil particles with a certain size d_{max} . (Figure 3b is derived from Figure 3a by truncating the particle size distribution of the soil, i.e., by eliminating particles greater than d_{max} , where d_{max} is such that the particles smaller than d_{max} form a soil with a coefficient of uniformity of 3.)

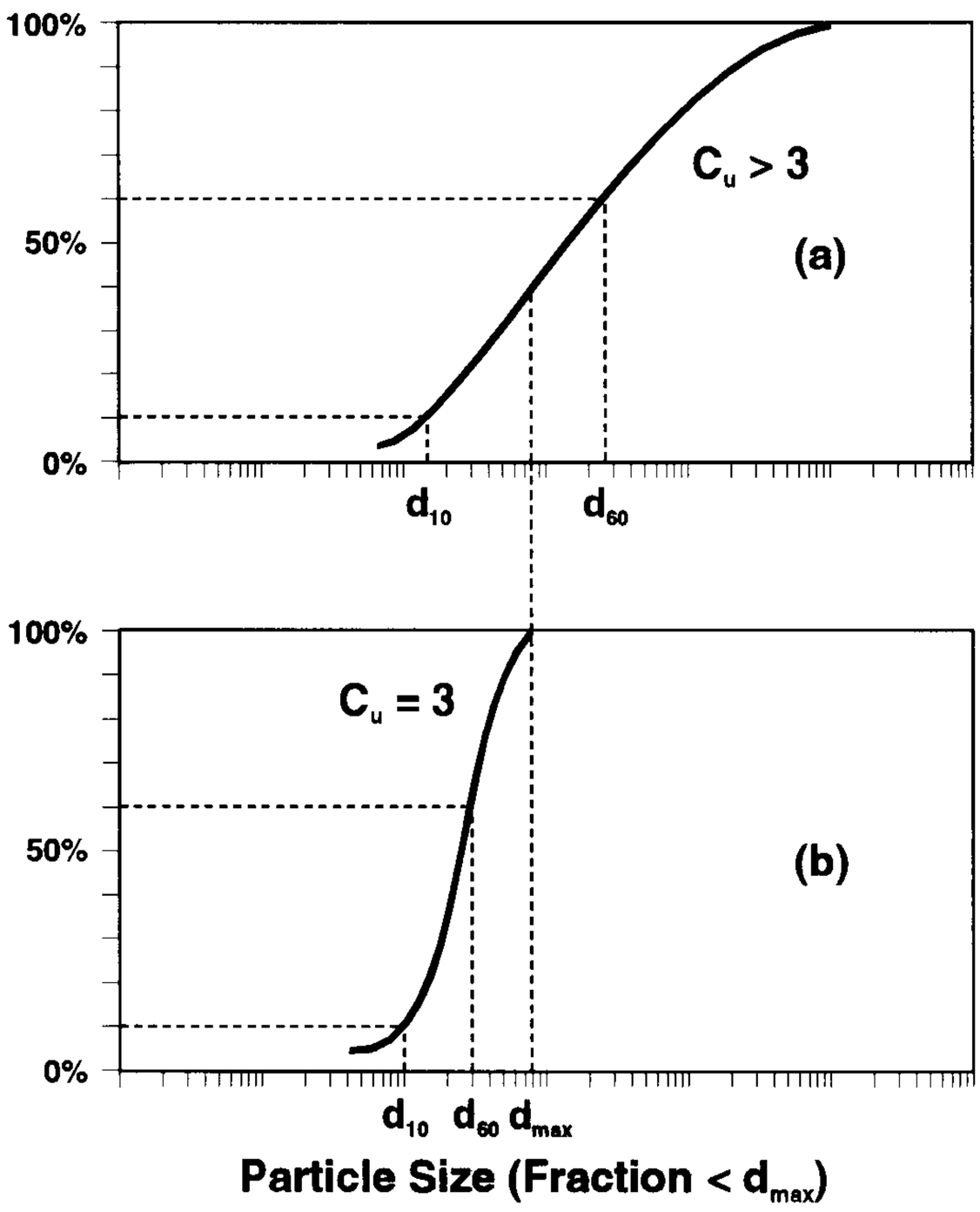

Fig. 3 Determination of the particle size that a geotextile filter should retain if the coefficient of uniformity of the soil is greater than 3: (a) particle size distribution of the soil; and (b) particle size distribution of the fraction of the soil that is internally stable.

In the above demonstration, the following expression was used several times: "selecting a filter that just retains soil particles with a size d". This expression implied, but did not exactly state, that such a filter should have its maximum openings equal to the soil particle size. In fact, this would be the case only for a loose soil. As shown below, larger openings could be used for a dense soil. Figure 4a shows schematically that, in the case of a loose soil represented by a cubic arrangement of spheres, if one particle goes through the filter opening, then all other particles can follow it. In contrast, in the case of a dense soil represented by an hexagonal arrangement of spheres, the soil structure remains stable if only one particle goes through the filter opening (Figure 4b); the structure becomes unstable only if two particles can pass simultaneously through a filter opening (Figure 4c). It therefore appears that, in the case of a loose soil, the filter openings must be just smaller than the size of the particle that the filter is intended to retain, whereas, in the case of the same soil in a dense state, the filter openings can be twice as large as the particles the filter is intended to retain. This conclusion can be considered conservative, because soil particles are not spherical and it seems logical to expect that non-spherical particles are less mobile, hence more stable, than spherical particles.

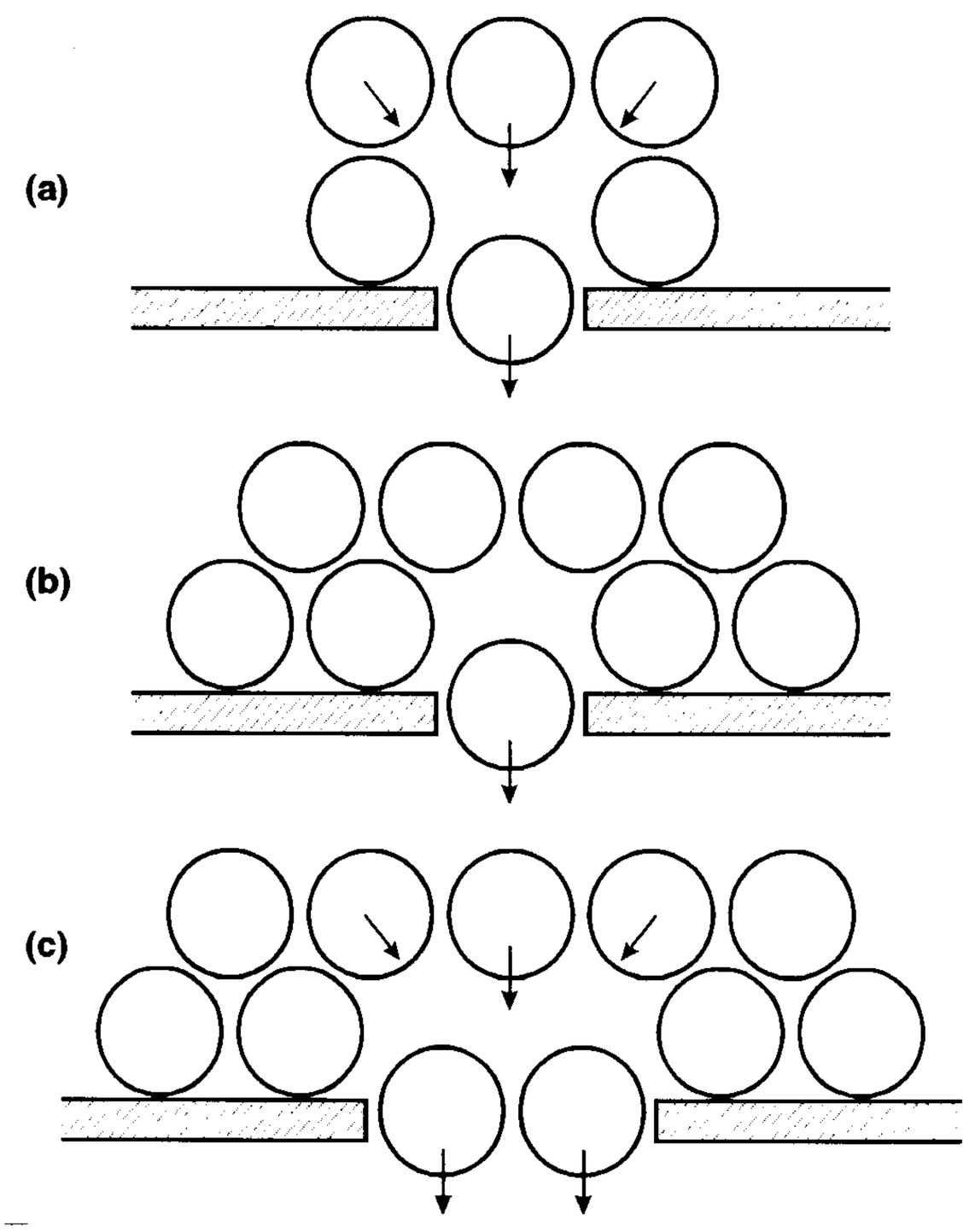

Fig. 4 Filter opening size as a function of soil density.

Two essential conditions were established in the above demonstrations:

- The filter must retain the largest soil particle of the fine fraction of the soil that has a coefficient of uniformity of 3 (i.e., d_{max} in Figure 3b).
- To retain particles of a certain size, the filter openings can be as large as the particle size if the soil is in a loose state and as large as twice the particle size if the soil is in a dense state.

Giroud (1982) has mathematically expressed the two

above conditions, assuming that the soil particle size distribution is a straight line in the usual axes, p-log d (where p is the percentage by mass of particles smaller than d), and therefore using a linear coefficient of uniformity, C_u' (equal, or close, to the coefficient of uniformity, C_u, in many cases). The retention criterion thus obtained is presented in Table 1 and Figure 5.

Table 1. Retention criterion for geotextile filters (Giroud, 1982).

	Density index of the soil (Relative density)	Linear coefficient of uniformity of the soil $1 < C_u' < 3$	$C_u' > 3$
loose soil	< 35%	$O_{95} < C_u' \, d_{50}$	$O_{95} < \frac{9}{C_u'} \, d_{50}$
medium dense soil	35 - 65%	$O_{95} < 1.5 \, C_u' \, d_{50}$	$O_{95} < \frac{13.5}{C_u'} \, d_{50}$
dense soil	> 65%	$O_{95} < 2C_u' \, d_{50}$	$O_{95} < \frac{18}{C_u'} \, d_{50}$

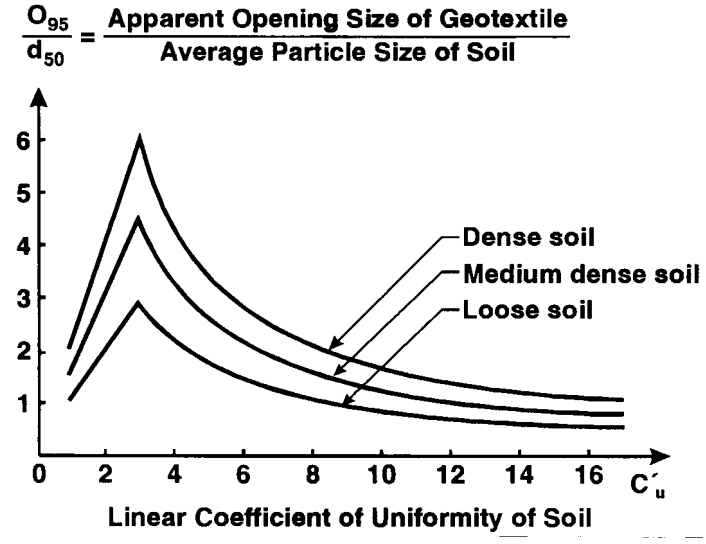

Fig. 5 Retention criterion for geotextile filters (Giroud, 1982).

It should be noted that the retention criterion given in Table 1 and Figure 5 is expressed as a function of the d_{50} of the soil. (d_{50} was selected by Giroud (1982) because it is far from both ends of the particle size distribution curve and, therefore, is not prone to experimental errors and is likely to be identical whether the coefficient of uniformity, C_u, or the linear coefficient of uniformity, C_u', is used.) The same mathematical process that leads to Table 1 can be used to express the retention criterion as a function of d_{85}, which makes it easier to compare with other criteria, generally expressed as a function of d_{85}. The retention criterion expressed as a function of d_{85} is given in Table 2 (Giroud, 1988) and Figure 6 (Giroud, 1982). Figure 6 shows a very important result. For values of the linear coefficient of uniformity of the soil, C_u', greater than 3.6 (loose soil) or 5.5 (dense soil), the required value of the geotextile opening size, O_{95}, is less than d_{85}. In these cases, it would be dangerous to design a filter using Equation 1: the soil would not be retained (unless it had a high cohesion). Figure 6 also shows that soils with a small coefficient of uniformity (i.e., soils that are naturally rather stable) are retained by filters that have openings larger than the largest soil particles.

Table 2. Retention criterion for geotextile filters (Giroud, 1988). Note: This criterion is identical to the criterion presented in Table 1, but it is expressed as a function of d_{85}.

	Density index of the soil (Relative density)	Linear coefficient of uniformity of the soil $1 < C_u' < 3$	$C_u' > 3$
loose soil	< 35%	$O_{95} < (C_u')^{0.3} \, d_{85}$	$O_{95} < \frac{9}{(C_u')^{1.7}} \, d_{85}$
medium dense soil	35 - 65%	$O_{95} < 1.5(C_u')^{0.3} \, d_{85}$	$O_{95} < \frac{13.5}{(C_u')^{1.7}} \, d_{85}$
dense soil	> 65%	$O_{95} < 2(C_u')^{0.3} \, d_{85}$	$O_{95} < \frac{18}{(C_u')^{1.7}} \, d_{85}$

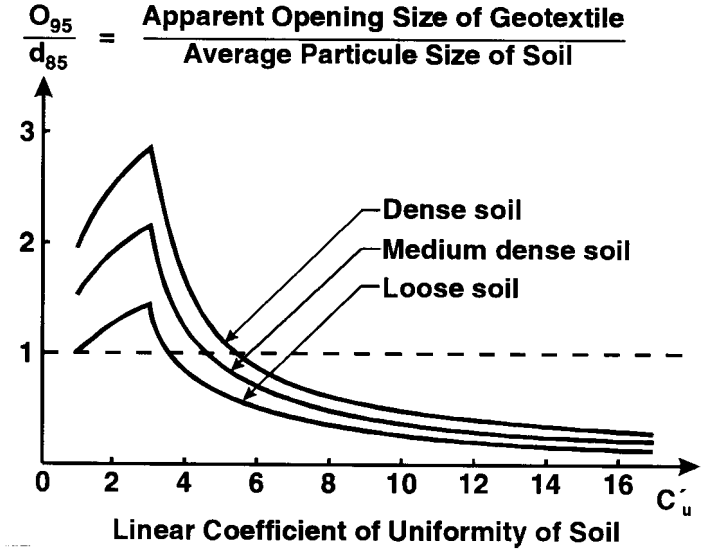

Fig. 6 Retention criterion for geotextile filters (Giroud, 1982). Note: This criterion is identical to the criterion presented in Figure 5, but it is expressed as a function of d_{85}.

2.3 Discussion

As mentioned above, following common sense that dictates to use a filter with openings smaller than the smallest soil particles is absurd, because it would lead to using quasi-impermeable filters (which, of course, would not meet the permeability criterion). In fact, the analysis presented above shows that, in some cases, the filter openings can be larger than the largest soil particles and the filter will still retain the soil.

The analysis presented above also shows that adapting rules used in geotechnical engineering for sand filters may be dangerous for geotextile filters, because they may lead to using geotextile filters with openings larger than they should be. This point deserves a comment. One may wonder why a simple rule successfully used for decades in geotechnical engineering for sand filters cannot be readily adapted to geotextile filters. First, it should be noted that geotechnical engineers know the limitations of their rules and correct them when necessary. For example, it is traditional in geotechnical engineering to ignore soil particles larger than 4.75 mm in the design of sand filters. This approach is similar to what was done in Figure 3, above, as part of the establishment of the geotextile filter retention criterion. However, there is a major difference: in the establishment of the geotextile filter criterion, the separation between the coarse fraction, which is ignored, and the fine fraction considered in the design is based on a rational consideration (i.e., the internal stability of the fine fraction), whereas the 4.75 mm separation traditionally used in geotechnical engineering is arbitrary. Furthermore, in the retention criterion for geotextiles, the separation of the soil particle size distribution in two parts (i.e., the truncation shown in Figure 3) is automatically included in the equations given in Tables 1 and 2. As a result, the user of the retention criterion for geotextiles does not have to truncate the particle size distribution of the soil. In fact, it is remarkable that, even if the user of the geotextile retention criterion truncates the particle size distribution of the soil, the calculated value of the filter opening size is unchanged (as shown by Giroud, 1988) because the filter criterion for geotextiles adjusts itself automatically to the truncated particle size distribution. In contrast, using the arbitrary 4.75 mm truncation procedure with Equation 1 (as recommended in some filter design methods) gives inadequate geotextile filter openings, generally too large and leading to a high risk of soil piping, as shown in an example presented by Giroud (1988).

At this point, one may wonder why the arbitrary 4.75 mm truncation procedure has been successful with sand filters and is not recommended for geotextile filters. The following explanation is proposed: it is possible that sand filters are more "forgiving" than geotextile filters for the following reason. If the filter openings are larger than they should be, some soil particles migrate. These particles are more likely to be entrapped in a sand filter than in a geotextile filter, because sand filters are much thicker than geotextile filters and their porosity (typically 30%) is less than that of geotextile filters (typically 90% for needlepunched nonwovens). As a result, the opening size of the sand filter decreases as soil particle migration occurs until an equilibrium is reached when the opening size of the partially clogged sand filter has reached the appropriate value required to retain the soil. In contrast, the geotextile being thin and having a large porosity is less likely to entrap particles or to be significantly modified by those entrapped. Clearly, the solution for geotextile filters is not to adopt some arbitrary rules traditionally used in geotechnical engineering, but to conduct a rational analysis, which leads to a strict retention criterion.

3 GEOTEXTILE FILTER CLOGGING

3.1 Overview

A geotextile filter can successfully retain a soil if the following conditions are met:

- the soil has a continuous particle size distribution (it is "well graded") and it is in a dense state, which ensures maximum interlocking of the soil particles;
- the geotextile filter openings are properly selected, as discussed in Section 2; and
- the soil is in close contact with the geotextile filter, so there is no open space between the soil and the geotextile where particles could move or accumulate.

The first two conditions were discussed in Section 2. The third condition is discussed below.

Even when the above conditions are met some soil particles move when water flows toward the filter: those few small particles that are at the surface of the soil, next to the filter, and, therefore, are not entrapped in the soil structure. More soil particles are displaced by the flow of water when the above conditions are not met.

Soil particles that are displaced by water flow may pass through the geotextile filter and migrate into the drain. If this is expected to happen, the drain should be designed to accommodate these particles. If the particles displaced by water do not pass through the filter, they interact with the filter in three different ways:

- Soil particles may form a thin layer (often called cake) at the surface of the filter. This mechanism is sometimes referred to as "blinding" of the filter.

- Individual soil particles may obstruct geotextile filter openings. This is possible in the case of filters with individual openings such as woven geotextiles. This mechanism is sometimes referred to as "blocking" of the filter.
- Soil particles may become entrapped within the filter. This is possible in the case of thick filters, such as needlepunched nonwoven geotextiles. This mechanism is sometimes referred to as "clogging" of the filter. However, the term "clogging" is also used to encompass the three mechanisms described above.

The modes of interaction between soil particles and geotextile filters have been described qualitatively in many publications. In this section, a method to quantify two of the mechanisms, blinding and clogging, is presented. Results obtained with this method lead to a number of practical conclusions, in particular on geotextile filter thickness, a point that is often discussed, but generally in qualitative terms.

3.2 Summary of the Theoretical Analysis

Darcy's law is not a law. In the mechanics of continua, a law is the simple mathematical expression of an experimental relationship between stresses, strains, and their derivatives with respect to time. Examples of laws are Hooke's law (elasticity) and Newton's law (viscosity). Combining fundamental equations of mechanics (force proportional to mass and acceleration) and mechanics of continua (continuity) with a given law, and integrating for certain boundary conditions, gives an equation that is the solution to the problem characterized by the considered boundary conditions. For example, integrating Newton's law of viscosity for a pipe gives Poiseuille's equation for laminar flow in pipes. Similarly, integrating Newton's law of viscosity for a permeable medium with a random organization (particles, fibers) gives Darcy's equation for laminar flow in permeable media. Clearly, Darcy's equation is not a law because it can be derived from a law. Equally clearly, Poiseuille's equation and Darcy's equation are similar and it should be possible to express both equations in similar ways, which can be achieved using the expression known as Kozeny-Carman's equation:

$$k = \frac{\lambda \rho_w g}{\eta_w} \frac{n^3}{(1-n)^2} \frac{1}{s_v^2} \quad (2)$$

where: k = hydraulic conductivity of the permeable medium; λ = shape factor function of the tortuosity of the medium; ρ_w = density of water; g = acceleration of gravity; η_w = viscosity of water; n = porosity of the permeable medium; and s_v = volumetric specific surface area of the permeable medium. In the case of a randomly organized permeable medium, the value λ = 0.1 can be used (Giroud, 1978). The volumetric specific surface area is:

$$s_v = 6/d_p \quad \text{for} \quad \text{spherical} \quad \text{particles} \quad (3)$$

$$s_v = 4/d_f \quad \text{for} \quad \text{fibers} \quad (4)$$

where: d_p = particle diameter; and d_f = fiber diameter.

With ρ_w = 1000 kg/m^3, g = 9.81 m/s^2 and $\eta_w = 10^{-3}$ kg/(m · s), Equations 2, 3 and 4 give:

$k = 4.8 \times 10^{-9}$ m/s for a clay (n = 0.4, d_p = 1 μm)

$k = 4.0 \times 10^{-3}$ m/s for a needlepunched nonwoven geotextile (n = 0.9, d_f = 30 μm)

It is then assumed that a quantity, m, of soil particles (expressed as a mass per unit area of filter) migrates from the soil and reaches the filter. Using Equation 2, it is possible to compare the case where the soil particles form a cake at the surface of the filter and the case where they accumulate inside the filter.

It is assumed that the soil contains a range of particle sizes, the smallest ones having an equivalent diameter of 1 μm, and it is assumed that only these small particles migrate toward the filter. If they accumulate at the surface of the geotextile filter to form a cake, the hydraulic conductivity of this cake will be 4.8×10^{-9} m/s as indicated above, which is a typical value for a layer of soil with clay-size particles.

If the soil particles accumulate inside the geotextile, two cases can be considered: the soil particles are uniformly dispersed in the pore space of the geotextile filter, or the soil particles agglutinate around the fibers. The theoretical analysis (Giroud, 1978) based on Equations 2, 3 and 4 gives the following equations:

$$k_1 = \frac{\lambda \rho_w g}{\eta_w} \frac{\left[n - \frac{m}{t_{GT} \rho_s} \right]^3}{\left[\frac{4(1-n)}{d_f} + \frac{6}{d_p} \frac{m}{t_{GT} \rho_s} \right]^2} \quad (5)$$

$$k_2 = \frac{\lambda \rho_w g}{\eta_w} \frac{\left[\frac{d_f}{4} \right]^2 \left[n - \frac{m}{t_{GT} \rho_s (1-n')} \right]^3}{(1-n) \left[1 - n + \frac{m}{t_{GT} \rho_s (1-n')} \right]} \quad (6)$$

where: k_1 = hydraulic conductivity of the partly clogged geotextile, assuming that the soil particles are uniformly dispersed in the pore space of the geotextile filter; k_2 = hydraulic conductivity of the partly clogged geotextile filter, assuming that the soil particles agglutinate around the fibers; m = mass of soil particles reaching the geotextile filter per unit area of geotextile; t_{GT} = geotextile thickness; ρ_s = density of soil particles; and n′ = porosity of the sheath of agglutinated soil particles.

It should be noted that Equation 6 was established using simplifying assumptions that limit its validity to cases where m is small compared to the value of m_{max} that corresponds to the case where soil particles fill all the geotextile filter pore space. A numerical application of Equations 5 and 6 is presented in Figure 7 for the following values of the parameters: porosity of the geotextile, n = 0.9; fiber diameter, d_f = 30 μm; soil particle diameter, d_p = 1 μm; porosity of the layer of soil particles when they form a blinding cake at the surface of the geotextile or when they agglutinate on geotextile fibers, n′ = 0.4; and, density of soil particles, ρ_s = 2700 kg/m^3.

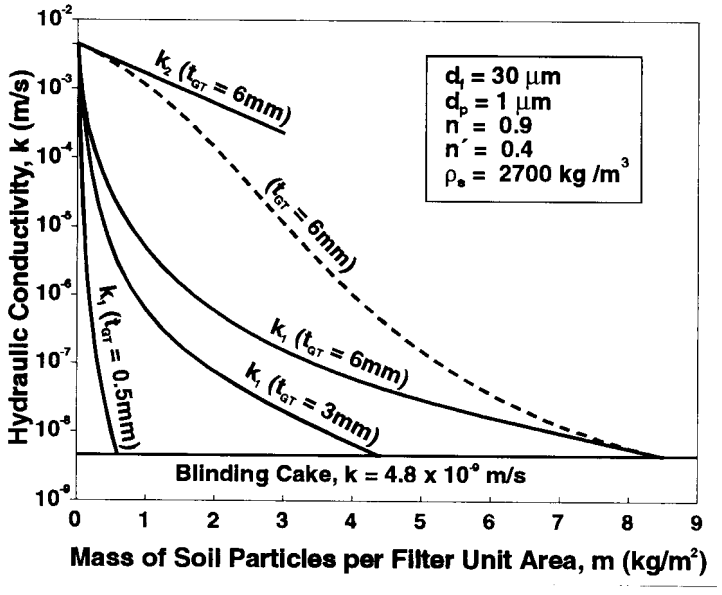

Fig. 7 Hydraulic conductivity of a geotextile filter as a function of the amount of soil particles entrapped in the geotextile: curves k_1 , obtained with Equation 5, represent the case where soil particles are uniformly dispersed in the geotextile pore space; curve k_2 , obtained with Equation 6, represent the case where soil particles agglutinate around geotextile fibers; and the dashed curve has been interpolated between the curves k_2 and k_1. Note: If the soil particles form a blinding cake at the surface of the geotextile, the permeability is constant and equal to 4.8 x 10^{-9} m/s.

Figure 7 shows that assuming that the soil particles are uniformly dispersed in the geotextile filter pore space (k = k_1) is more conservative than assuming that they agglutinate around fibers (k = k_2). It is likely that, for small values of m, the actual curve is close to the curve related to the assumption of agglutinated particles, and, for increasing values of m, progressively tends toward the curve obtained assuming that the particles are uniformly dispersed in the geotextile pore space. Accordingly, the actual curve is tentatively shown with a dashed line in Figure 7 for the case where the geotextile filter thickness is 6 mm.

3.3 Discussion

Figure 7 shows that a geotextile filter remains rather permeable even if a significant amount of soil particles accumulate inside the filter. This effect is most marked if the geotextile filter is thick. Therefore, the method presented above may provide a means to justify the use of thick geotextile filters in cases where soil particle migration is expected.

It is also clear from Figure 7 that blinding (i.e., formation of a cake of fine particles at the surface of a geotextile filter) is far more detrimental than clogging (i.e., accumulation of particles within the filter). Therefore, it is imperative that geotextile filters be placed in intimate contact with the soil, as it may be expected that, if this condition is met, blinding will not develop for the following two reasons:

- There may not be enough space for the cake of small soil particles to develop at the surface of the geotextile if the geotextile and soil are in intimate contact.
- The soil particles being immediately retained by the geotextile filter do not move (with the exception of some small soil particles located in front of geotextile openings), whereas if there is a space between the geotextile filter and the soil, all soil particles have to move before they can be retained by the geotextile filter. The disorganization of the soil structure associated with this movement makes it possible for more soil particles to move and reach the filter.

It is also possible that geotextiles with a tortuous surface in contact with the soil, such as needlepunched nonwoven geotextiles, do not favor the development of a continuous cake of fine soil particles, whereas geotextile filters with a smooth surface may favor the development of such a cake. Furthermore, geotextiles with a tortuous surface do not favor the mechanism of blocking, which was mentioned in Section 3.1, because they do not have individual openings.

4 GEOMEMBRANE STRESS-STRAIN BEHAVIOR

4.1 Overview

Geomembranes are essential, but weak, components of containment structures. They have to withstand stresses and/or displacements imposed on them, but they are not expected to contribute to the mechanical behavior of the structure. Whether they are subjected to gravity stresses on slopes (imposed stresses) or to differential settlements (imposed displacements), it is important to know their mechanical characteristics to quantify their behavior. The example of high density polyethylene (HDPE) geomembranes will be used to illustrate the nature of the relevant information.

Historically, HDPE geomembranes have been portrayed as superior to others because their 800% strain at break would preclude any failure in containment structures where such large strains virtually never exist. However, after a few failures and after it was demonstrated (Giroud, 1984a, 1984b) — and vigorously proclaimed — that failures in actual field conditions are governed by the yield strain (on the order of 10%), engineers started using the yield strain to design applications of HDPE geomembranes. Regrettably, however, the yield strain of geomembranes is often not properly measured. Tensile tests must be performed with an extensometer to measure the tensile strain in the central, narrow portion of the geomembrane dumbbell specimen. Instead, the strain is often derived from grip separation, which can overestimate the yield strain by as much as 50%, as shown by Giroud et al. (1994a).

Engineers have always recognized that uniaxial tensile tests (such as those performed on dumbbell specimens) do not represent field situations where stress states in geomembranes are biaxial or even triaxial. To meet this need, many testing laboratories perform "axi-symmetric multiaxial hydrostatic" tests, where a circular geomembrane specimen is inflated with air or water. The curve of the geomembrane deflection versus the inflation pressure is measured and a stress-strain curve is mathematically derived assuming that the shape of the deformed geomembrane is spherical. However, the shape of the deformed geomembrane cannot be a sphere, because the stress state is biaxial isotropic at the apex of the dome formed by the geomembrane and is of the plane strain type at the circular periphery ($\epsilon_\theta = 0$, $\epsilon_r \neq 0$, ϵ_θ being the circumferential strain and ϵ_r the radial strain), whereas a spherical shape can only result from an isotropic biaxial stress state everywhere in the specimen. As a result, the stresses are greater at the apex of the dome than anywhere else in the specimen and a geomembrane subjected to the axi-symmetric multiaxial hydrostatic test always fail at the apex of the dome (unless the geomembrane has a defect located somewhere else). Because the shape of the deformed geomembrane is not spherical, the stresses and strains in the geomembrane are different from those calculated assuming a spherical shape. As a result, the interpretation of axi-symmetric multiaxial hydrostatic tests is questionable and the stress-strain curves derived from axi-symmetric multiaxial hydrostatic tests are typically not used in design calculations.

From the above overview, it appears that the state of practice is not satisfactory and that the data typically offered to engineers are not the most appropriate data for design. As shown in the summary presented below, appropriate data are available, at least for HDPE geomembranes.

4.2 Summary of Data

Manufacturers and testing laboratories typically provide the complete stress-strain curve of HDPE geomembranes (Figure 8a), whereas a close-up view of the initial portion of the curve (Figure 8b) would be more useful

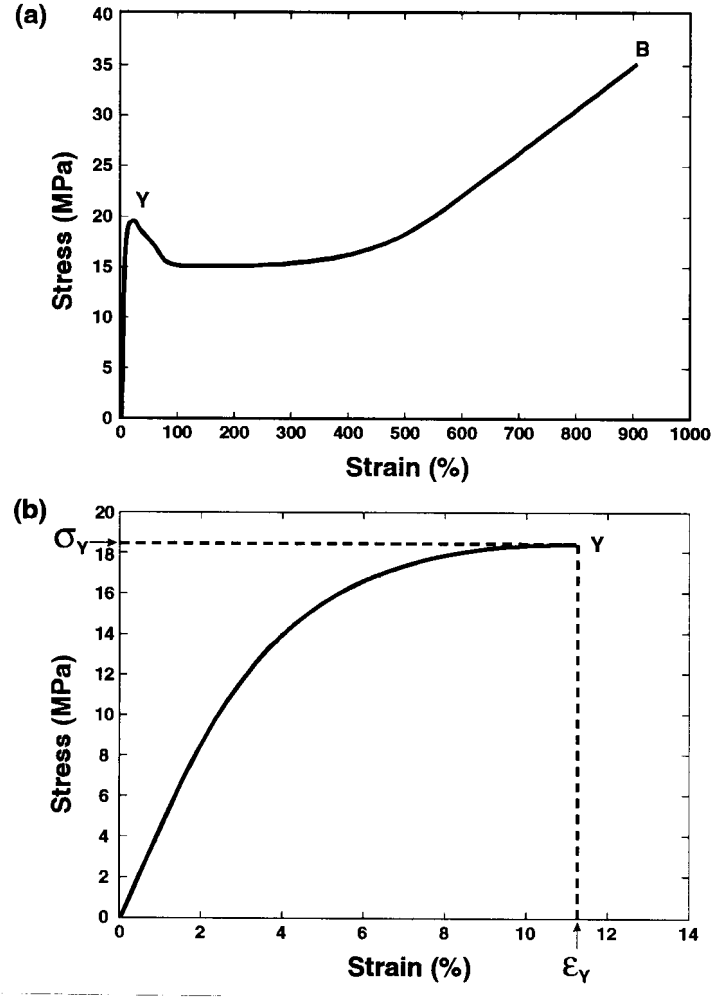

Fig. 8 Typical uniaxial stress-strain curve of an HDPE geomembrane: (a) entire curve from the origin to the break point, B; and (b) initial portion of the curve from the origin to the yield peak, Y.

to the design engineer since, as discussed above, the yield strain, not the strain at break, should be considered in design. It appears on Figure 8b, that the portion of an HDPE geomembrane stress-strain curve between the origin and the yield peak is far from being a straight line, as one may wrongly assume from observing the curve given in Figure 8a.

To provide design engineers with complete data on the tensile behavior of HDPE geomembranes, more than 500 tensile tests were conducted on HDPE geomembrane specimens from five U.S. manufacturers, at temperatures ranging from -20°C to 70°C (Giroud et al., 1993). Geomembrane thicknesses ranged from 0.5 to 3 mm. The tests were conducted on dumbbell specimens according to ASTM Standard Test Method D 638, at a speed of 50 mm/minute with geomembrane elongations measured using an extensometer.

The tests did not show large differences between the stress-strain curves for HDPE geomembranes from different manufacturers. Figure 9a presents the average stress-strain curves obtained for HDPE geomembranes at each testing temperature, i.e., each stress-strain curve in Figure 9a was obtained by averaging stress-strain curves from all tests conducted at that temperature on all HDPE specimens included in the testing program, regardless of manufacturer. Only the portions of the stress-strain curves between the origin and the yield peaks are shown in Figure 9a.

Average values of the yield stress, σ_Y , and the yield strain, ϵ_Y , obtained at various temperatures are given in Figures 9b and 9c, respectively. (Values outside the -20°C to 70°C range were extrapolated.) Inspection of Figure 9b indicates that the relationship between σ_Y and temperature is virtually linear. Also, $\sigma_Y = 0$ at the temperature of fusion of HDPE (140°C), which is logical. Figure 9c shows that ϵ_Y tends toward infinity for the temperature of fusion of HDPE, which is logical too.

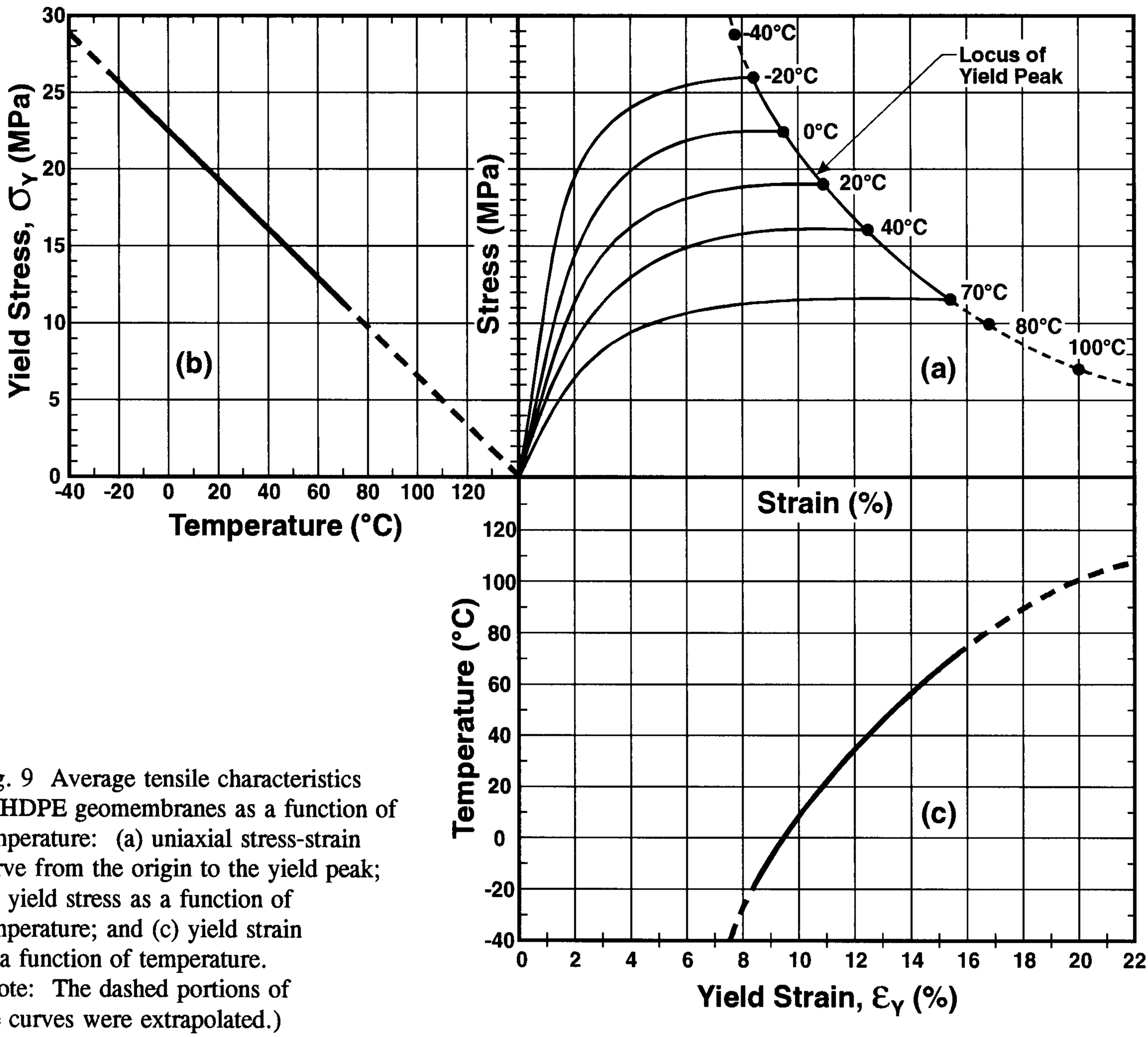

Fig. 9 Average tensile characteristics of HDPE geomembranes as a function of temperature: (a) uniaxial stress-strain curve from the origin to the yield peak; (b) yield stress as a function of temperature; and (c) yield strain as a function of temperature. (Note: The dashed portions of the curves were extrapolated.)

Another useful result from the testing program is the curve giving the initial modulus of HDPE geomembranes as a function of temperature (Figure 10). It should be noted that the modulus is zero at the temperature of fusion of HDPE.

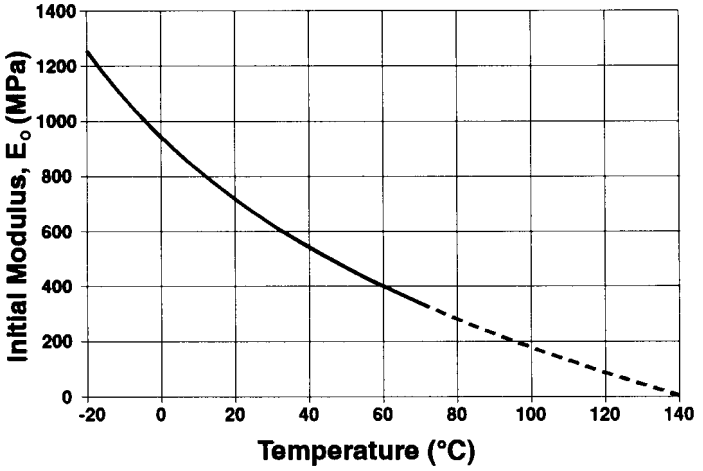

Fig. 10 HDPE geomembrane initial uniaxial modulus as a function of temperature. The portion of the curve represented by a dashed line has been extrapolated.

A remarkable result was obtained from the testing program: the average stress-strain curves for HDPE geomembranes at different temperatures become nearly identical when presented in normalized axes, σ/σ_Y and ϵ/ϵ_Y . (It is possible that this result stems from a fundamental rheological trait of HDPE, but this was not investigated.) Furthermore, it has been shown that the normalized average stress-strain curve (i.e., the unique normalized stress-strain curve that represents with a good approximation all tested HDPE geomembranes regardless of temperature) can be represented by an n-order parabola (Giroud, 1994a), the equation of which is:

$$\sigma/\sigma_Y = 1 - (1 - \epsilon/\epsilon_Y)^n \qquad (7)$$

An excellent approximation of the normalized average stress-strain curve from the testing is obtained with Equation 7 when n = 4 (Figure 11). Knowing only the stress and strain at the yield peak of a given HDPE geomembrane for a given temperature, Equation 7, with n = 4, gives the stress-strain curve of the geomembrane between the origin and the yield peak at that temperature. If the stress and strain at the yield peak are not known, they can be obtained from Figures 9b and 9c, since the testing program did not show large differences between the stress-strain curves of various HDPE geomembranes, as mentioned above. Therefore, with the n-order parabola (Equation 7), it is possible to describe in a quantitative manner the portion of the stress-strain curve that is relevant to the design of HDPE geomembrane applications. This has major design consequences.

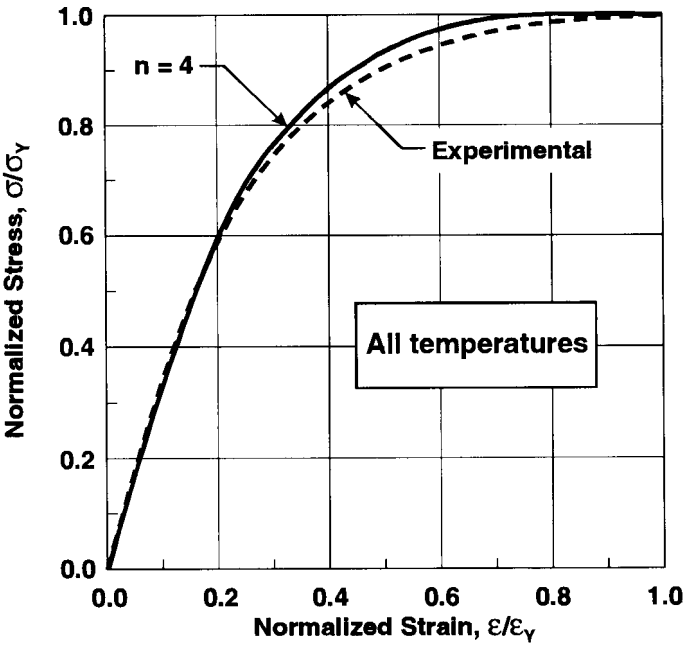

Fig. 11 HDPE geomembrane normalized uniaxial stress-strain curve. The theoretical curve (solid line) was obtained using Equation 7 with n = 4. The experimental curve is derived from Figure 9a.

The above results are related to smooth HDPE geomembranes. Systematic tests conducted with geomembranes textured using various processes gave results close to the above results for the portion of the stress-strain cures between the origin and the yield peak. With some textured geomembranes, tensile properties beyond the yield peak, in particular the stress and strain at break, were significantly different from the corresponding tensile properties for smooth geomembranes. However, the difference has no impact on design since the portion of the stress-strain curve that is relevant to design is the portion before the yield peak.

From Equation 7, it is possible to derive relationships between the secant and tangent moduli for any strain below the yield strain and the secant modulus at yield (Giroud, 1994a). Equations are not given here, but the relationships are presented in Figure 12.

An important consequence of the n-order parabola equation is that the initial modulus of an HDPE geomembrane, E_o , is n times the secant modulus at yield:

$$E_o = n\, E_{secY} = n\, \sigma_Y/\epsilon_Y \qquad (8)$$

and, if n = 4:

$$E_o = 4\, E_{secY} = 4\, \sigma_Y/\epsilon_Y \qquad (9)$$

This result is extremely useful because the initial modulus is not easy to measure, and not always provided, whereas the yield stress, σ_Y , and the yield strain, ϵ_Y , are routinely measured and readily available to the design engineer.

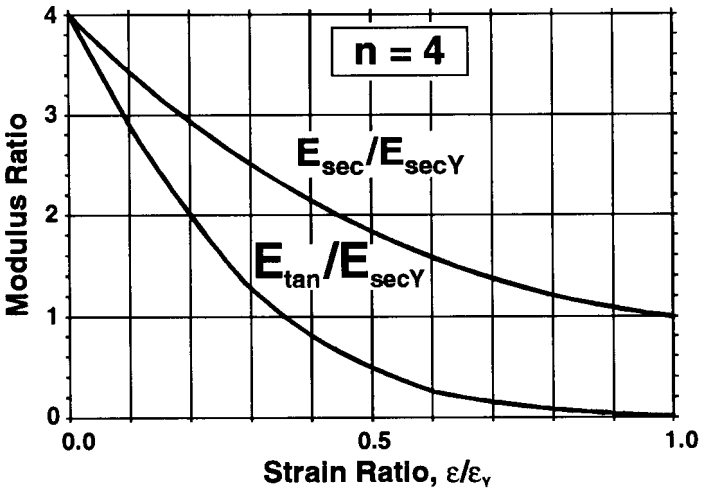

Fig. 12 HDPE geomembrane uniaxial secant and tangent moduli at any strain below the yield strain as a function of the secant modulus at yield. (E_{sec} = secant modulus at strain ϵ; E_{tan} = tangent modulus at strain ϵ; E_{secY} = secant modulus at yield, i.e., at strain ϵ_Y .)

Combining the results provided in Figures 10 and 12 gives the geomembrane modulus at any temperature and any strain for typical HDPE geomembranes.

All the results presented above where obtained from uniaxial tests. In the field, geomembranes are generally subjected to biaxial or triaxial stress states. In the case of biaxial stress states, which exist in the case of uncovered geomembranes, two cases are typically considered: the isotropic biaxial stress state, characterized by two equal stresses in the plane of the geomembrane ($\sigma_1 = \sigma_2$, $\sigma_3 = 0$), and the plane strain biaxial stress state, characterized by a zero strain in one direction of the geomembrane plane ($\sigma_1 \neq \sigma_2$, $\sigma_3 = 0$, $\epsilon_2 = 0$). An analysis based on energy conservation has led to relationships between uniaxial and biaxial stresses and strains in geosynthetics as a function of the Poisson's ratio, ν, of the geosynthetic (Soderman and Giroud, 1994). In the case where $\nu = 0.5$, which is relevant to unreinforced geomembranes, the following relationships were established:

$$\frac{\sigma_{Yib}}{\sigma_{Yu}} = 1 \quad \frac{\epsilon_{Yib}}{\sigma_{Yu}} = 0.5 \quad \frac{E_{ib}}{E_u} = 2 \qquad (10)$$

$$\frac{\sigma_{Yps}}{\sigma_{Yu}} = 1.15 \quad \frac{\epsilon_{Yps}}{\epsilon_{Yu}} = 0.87 \quad \frac{E_{ps}}{E_u} = 1.33 \qquad (11)$$

where: σ_Y = yield strain, ϵ_Y = yield strain, and E = modulus (which can be the initial modulus or the secant modulus at any given strain, provided that moduli at the same strain are used in numerator and denominator); and where the subscripts are: ib = isotropic biaxial stress state, ps = plane strain biaxial stress state, and u = uniaxial stress state.

These relationships are represented in Figure 13. The following comments can be made from Figure 13:

- Stress-strain curves obtained from an isotropic test (such as the axi-symmetric multiaxial hydrostatic test) are far too steep to adequately represent the plane strain biaxial stress state, which occurs more often in the field than the isotropic biaxial stress state.
- The yield stress of an unreinforced geomembrane is not very different in a biaxial and a uniaxial state of stress.
- The yield strain of an unreinforced geomembrane is significantly less in a biaxial state of stress than in a uniaxial state of stress.

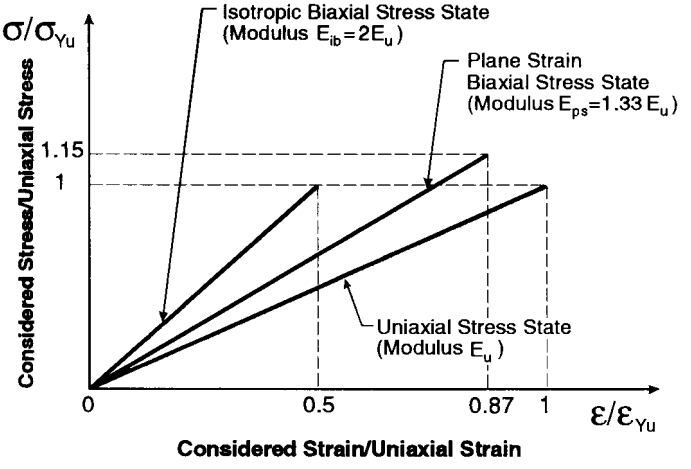

Fig. 13 Relationships between uniaxial and biaxial stress-strain curves of unreinforced geomembranes (Soderman and Giroud, 1994).

4.3 Discussion

The data presented above provide the design engineer with a complete set of information on HDPE geomembranes:

- stress-strain curves, including values of initial modulus, yield stress and yield strain, as a function of temperature;
- equation of the stress-strain curve valid at any temperature;
- variation of the secant and tangent moduli as a function of the strain; and
- relationships that make it possible to derive tensile characteristics of geomembranes (not only HDPE) in a biaxial stress state from tensile characteristics measured in a uniaxial test.

A design engineer, working with a certain HDPE geomembrane, may use the above set of generic data (potentially complemented by specific data on the considered geomembrane, such as the measured yield stress and yield strain) to obtain, for example, the modulus of the geomembrane in a biaxial stress state more accurately than by trying to interpret an axi-

symmetric multiaxial hydrostatic test on the considered geomembrane.

The development of similar data for all types of geomembranes is encouraged, which would promote rational design of geomembrane applications.

5 GEOMEMBRANE STRAIN CONCENTRATIONS

5.1 Overview

Geomembrane failures often occur at the edge of seams even though the seam itself does not fail. An example is discussed in Section 6, another is illustrated in Figure 14. In most cases, the failure of the geomembrane occurs at the connection between the seam and the "lower" geomembrane, as shown in Figure 15.

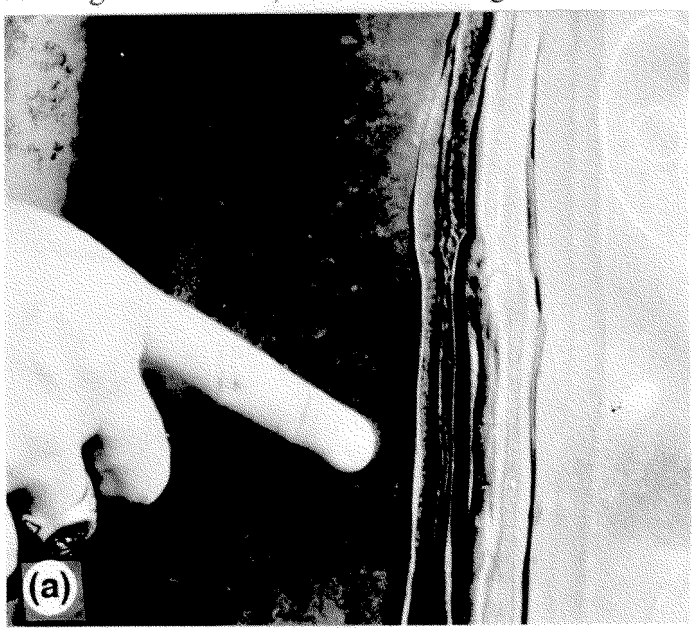

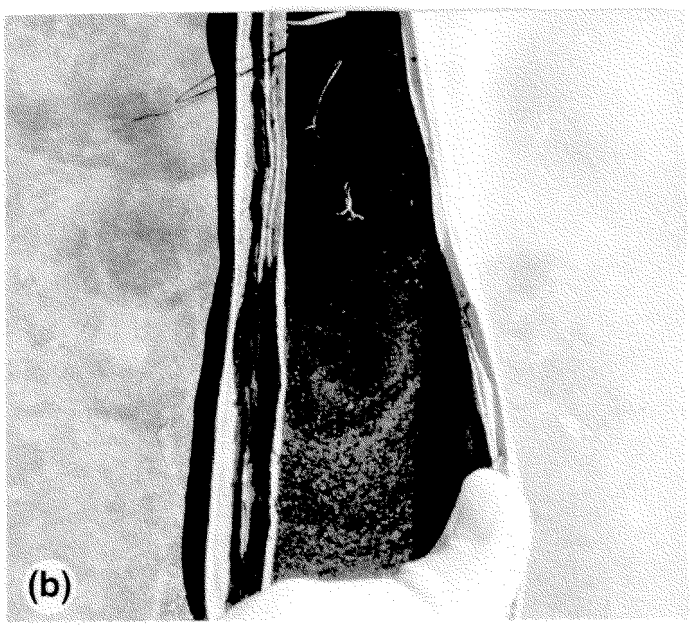

Fig. 14 Typical geomembrane failure next to a seam: (a) view of the crack as it appears along the seam; and (b) crack opened by hand.

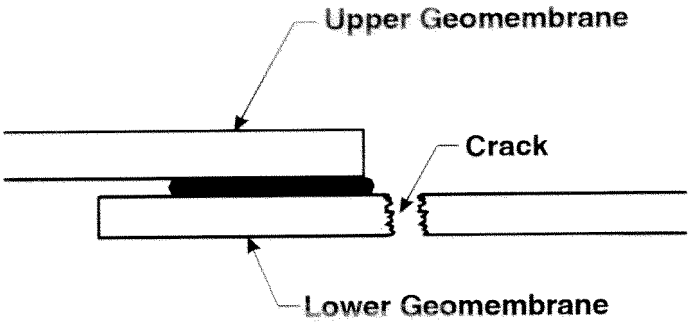

Fig. 15 Typical failure in the lower geomembrane.

The weakness of a geomembrane liner next to a seam may be due to a weakening of the geomembrane that results from the seaming process, e.g., overheating of the geomembrane causing structural changes in the geomembrane polymer, overheating of the geomembrane causing permanent deformations of the geomembrane in the vicinity of the seam likely to cause stress/strain concentrations in the geomembrane, overheating and/or excessive pressure causing a reduction in geomembrane thickness next to the seam, and improper grinding of the geomembrane as part of seam preparation for certain types of seams (e.g., extrusion fillet seams) causing a reduction in geomembrane thickness next to the seam. However, even if none of the above occurs, a geomembrane liner may fail next to a seam as a result of stress/strain concentrations that are simply due to the geometry of the seam itself.

Stress and strain concentrations are linked and either one can be used in an analysis. Herein, strain concentration is used because strains are dimensionless and, therefore, easier to use than stresses.

Strain concentration in a geomembrane may also be cause by localized lack of geomembrane thickness, which may be due to a variety of causes such as: (i) scratches due to carelessness during geomembrane installation or facility operation; (ii) excessive grinding during seam preparation, i.e., grinding that extends beyond the seamed area and, therefore, remains visible after the seam is made; (iii) overheating and excessive pressure next to a seam during seaming; and (iv) imprinting of a hard geonet into a softer geomembrane, under overburden loads. As this list suggests, in many cases, localized lack of geomembrane thickness occurs next to seams and, in these cases, the strain concentration due to the localized lack of thickness is added to strain concentration that results from the geometry of the seam.

The theoretical analysis that is summarized in Section 5.2 provides first an evaluation of the strain concentration that results from the geometry of a seam, and, then, an evaluation of the strain concentration that results from localized lack of thickness.

5.2 Summary of the Theoretical Analysis

As shown by Giroud (1984a, 1984b), seams rotate when a geomembrane is in tension because the equilibrium of the tensile forces applied on the geomembrane requires the portion of geomembrane on one side of a seam to be in the same plane as the portion of geomembrane on the other side of the seam. As a result, the geomembrane bends on each side of the seam (Figure 16). A detailed analysis of the bending of the geomembrane has been performed by Giroud et al. (1995). The analysis shows that the maximum tensile strain due to bending occurs at the connection between the geomembrane and the seam, i.e., either at A or B in Figure 16. Therefore, from the viewpoint of strain concentrations due to bending, failure of the geomembrane is equally possible at A or B (Figure 16). However, failure generally occurs at A (see Figure 15) because of one or both of the following reasons: (i) if failure occurs when the geomembrane liner is exposed to a low temperature, which is often the case, and results from tensile stresses due to restrained thermal contraction (i.e., contraction that cannot take place because the geomembrane is not free to move), the exposed face of the geomembrane (where point A is located) is colder than the face of the geomembrane in contact with the underlying soil and, as a result, is subjected to more thermal contraction; and (ii) the top face of the lower geomembrane in the vicinity of point A is more likely to be damaged (scratched) during installation than the bottom face of the upper geomembrane, in particular if grinding is used for geomembrane preparation to seaming.

The analysis provides equations to determine the maximum tensile strain due to bending as a result of the following parameters: geomembrane thickness, geomembrane modulus, seam type, seam thickness (in the case of extrusion seams), seam width, and the average tensile strain in the geomembrane that causes bending next to the seam. The equations are too numerous and complex to be reproduced here. However, in Figure 17, the maximum tensile strain due to bending is given in graphs for two geomembrane thicknesses and for several different types of seams (Figure 18).

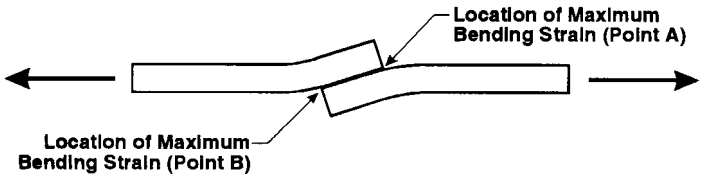

Fig. 16 Geomembrane bending on each side of a seam.

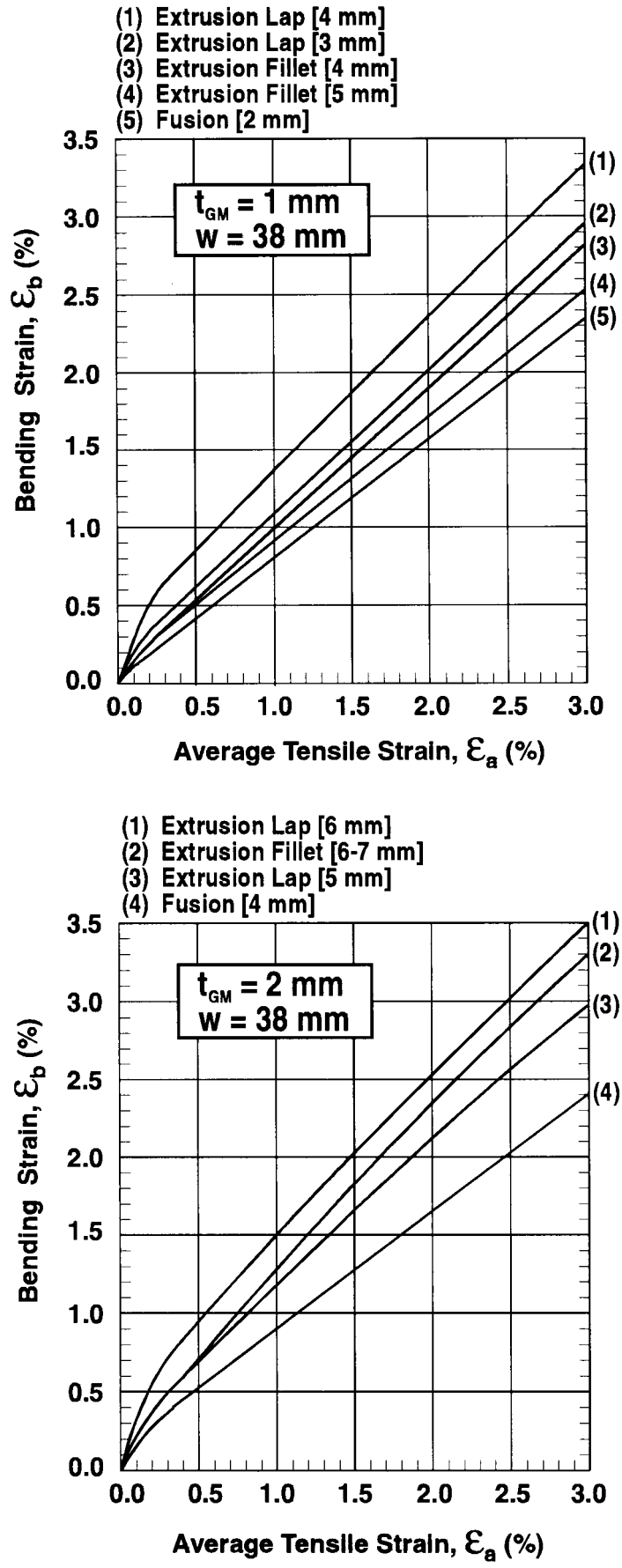

Fig. 17 Tensile strain due to geomembrane bending next to a seam, ϵ_b , as a function of the average tensile strain, ϵ_a , in the geomembrane (Giroud et al., 1993). Notes: The value indicated in square brackets is the total seam thickness, i.e., thickness of extrudate, if any, plus thickness of two geomembrane layers; t_{GM} = geomembrane thickness; and w = seam width.

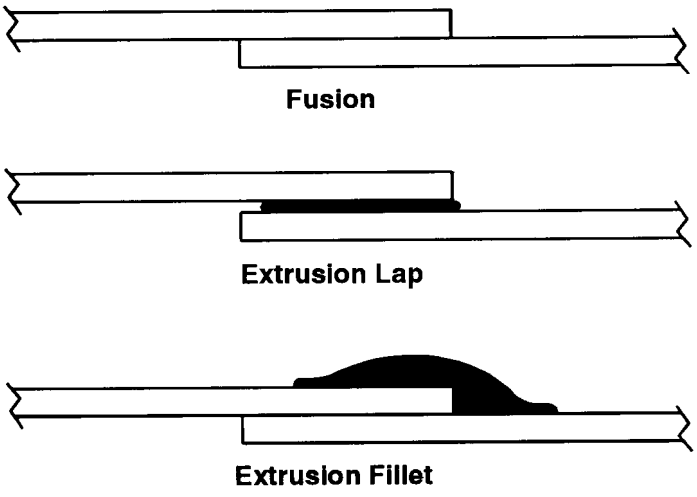

Fig. 18 Seam types.

In comparison with the complex analysis used to evaluate the strain concentration due to the geometry of seams, the evaluation of strain concentration due to a decrease of geomembrane thickness is simple. In fact, the stress concentration is proportional to the thickness reduction and, if the geomembrane stress-strain curve were linear, the strain concentration would also be proportional to the thickness reduction. However, geomembrane stress-strain curves are not linear. As indicated in Section 4.2, the stress-strain curve of an HDPE geomembrane can be represented by an n-order parabola. Figure 19 shows that, given the shape of the geomembrane stress-strain curve, a small thickness reduction (which causes an equally small stress concentration) causes a relatively large strain concentration, especially in the vicinity of the yield peak.

Giroud et al. (1994b) have shown that the ratio between the yield strain of a scratched geomembrane, ϵ_{Ys}, and the yield strain of an intact geomembrane, ϵ_Y, is given by the following equation derived from Equation 7:

$$\frac{\epsilon_{Ys}}{\epsilon_Y} = 1 - (d_s/t_{GM})^{1/n} \qquad (12)$$

where: d_s = depth of scratch or any other type of thickness reduction; and t_{GM} = geomembrane thickness (outside the zone of thickness reduction). The exponent n is generally equal to 4, as discussed after Equation 7. Equation 12, with n = 4, is represented in Figure 20.

5.3 Discussion

Figure 17 shows that the tensile strain due to bending is less for fusion seams than for extrusion seams. This is because extrusion seams are thicker than fusion seams. However, even for fusion seams, the tensile strain due to bending is significant: it is equal to approximately 80% of the average tensile strain in the geomembrane. In other words, the total tensile strain next to a fusion seam (i.e., the sum of the average tensile strain and the maximum tensile strain due to bending) is equal to 1.8 times the average tensile strain in the geomembrane. It has also been shown by Giroud et al. (1995) that seams narrower than those considered in Figure 17 would generally give greater strain concentrations. An important result of the theoretical analysis is that significant bending strains occur even though the seam rotation angle is small (typically only a few degrees). However, it should be noted that the method presented in Figure 17 is valid only in the case of seams that are

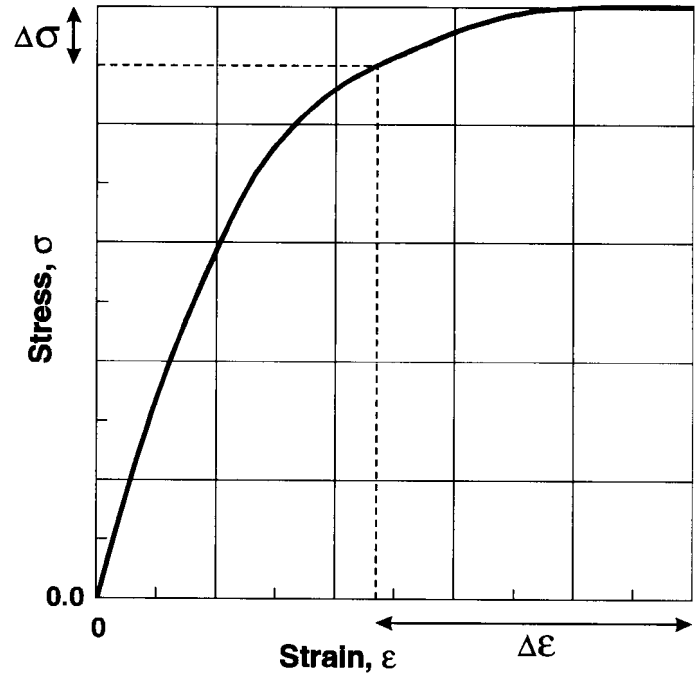

Fig. 19 Stress increase, $\Delta\sigma$, and strain increase, $\Delta\epsilon$, due to a 10% geomembrane thickness decrease.

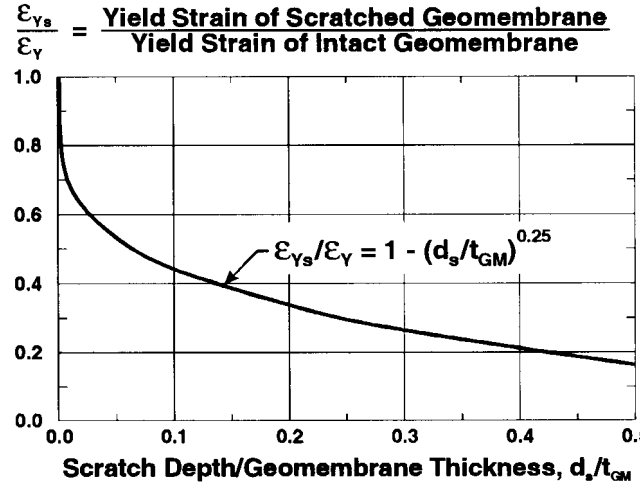

Fig. 20 Ratio of the yield strains of an HDPE geomembrane with a scratch, or any other type of thickness reduction, and an intact HDPE geomembrane (Giroud et al., 1993).

free to rotate; in the case of seams that are subjected to normal stresses (due to overlying materials) which limit their ability to rotate, the bending strain should be less than indicated in Figure 17. Therefore, exposed geomembranes are more prone than buried geomembranes to stress/strain concentration due to seam geometry.

The same type of analysis explains why geomembranes may fail next to abrupt changes in thickness. This is the case in particular with geomembranes produced using a manufacturing process that overlaps adjacent strips while in molten state. The area with a slightly greater thickness causes a strain concentration similar to that caused by a seam. An example of such failure is shown in Figure 21.

Fig. 21 Crack in an HDPE geomembrane located partly along a seam and partly along an area of greater thickness resulting from the manufacturing process.

Figure 20 shows that the strain concentration caused by a scratch, or any other type of thickness reduction, can be significant. It is not surprising that this mechanism has been at the origin of a number of failures of HDPE geomembrane liners, as pointed out by Giroud (1993). It is therefore necessary to take precautions to minimize the risk of scratching geomembranes, in particular next to seams, where the resulting strain concentration would be added to that resulting from the geometry of the seam. In particular it is recommended that grinding be done gently and in a direction perpendicular to the seam direction, in spite of the natural tendency to grind in a direction parallel to the seam. Also, grinding should not extend beyond the area to be seamed.

On the basis of strain concentrations due to the geometry of seams and the risk of localized thickness reduction, and using the methods presented in Section 5.2, the design engineer may determine the design yield strain of an HDPE geomembrane. The detailed procedure has been described by Giroud et al. (1993).

Finally, at a fundamental level, the following comment can be made: the fact that some textured HDPE geomembranes (depending on their manufacturing process) exhibit, in a standard uniaxial laboratory tensile test, a strain at break less than the strain at break of a smooth HDPE geomembrane (see Section 4.2) is consistent with the detrimental effects of surface irregularities (thickness reduction as well as extra thickness) mentioned above. (It should be noted that premature failures of some textured geomembranes in standard laboratory tests have no impact on their mechanical behavior since these failures occur beyond the yield strain.)

6 GEOMEMBRANE STRESS CRACKING PATTERN

6.1 Overview

High density polyethylene (HDPE) geomembranes may be susceptible in varying degrees to stress cracking, most likely as a function of the type of resin used in their manufacturing. Liners made with geomembranes that are susceptible to stress cracking sometimes exhibit "shattering cracks", i.e., cracks that develop in several directions, leaving a shattered geomembrane.

Shattering cracks have been typically observed on the side slopes of empty ponds where the geomembrane is anchored at the crest and is not free to move at the toe because of the presence of sediments and ice at the bottom of the pond. In a number of cases, after very low temperatures had occurred, the shattering cracks have been observed to form a quasi-symmetrical pattern on both sides of a straight crack (the "central crack") located along a seam (Figures 22 and 23). In such cases, careful observations have also shown the presence of geomembrane wrinkles oriented in directions that are approximately perpendicular to the directions of the shattering cracks. The observations are summarized in Figure 24. It should be noted that the extent of the phenomenon can be considerable. For example, in the case of slope that is 20 m long from crest to toe, the central crack would be 20 m long and the shattering cracks could extend 10 to 30 m to each side of the central crack.

The magnitude and the complexity of the crack pattern have impressed and intrigued observers and the presence of a central crack and wrinkles have raised questions:

- The presence of the central crack perpendicular to the

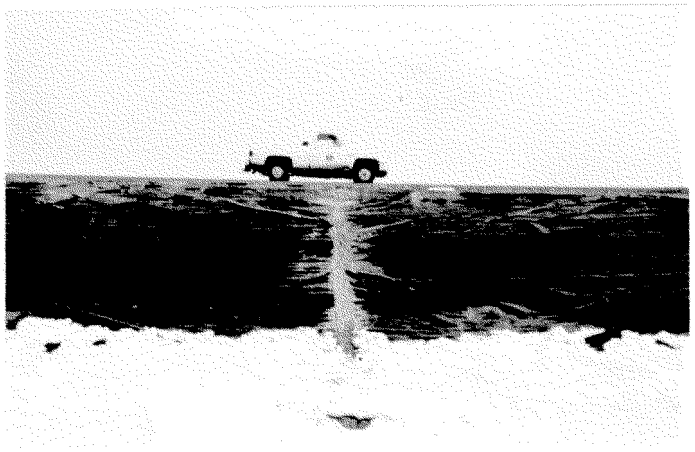

Fig. 22 Quasi-symmetrical pattern of shattering cracks associated with a crack located along a seam ("central crack") in the case of a geomembrane exposed on a slope.

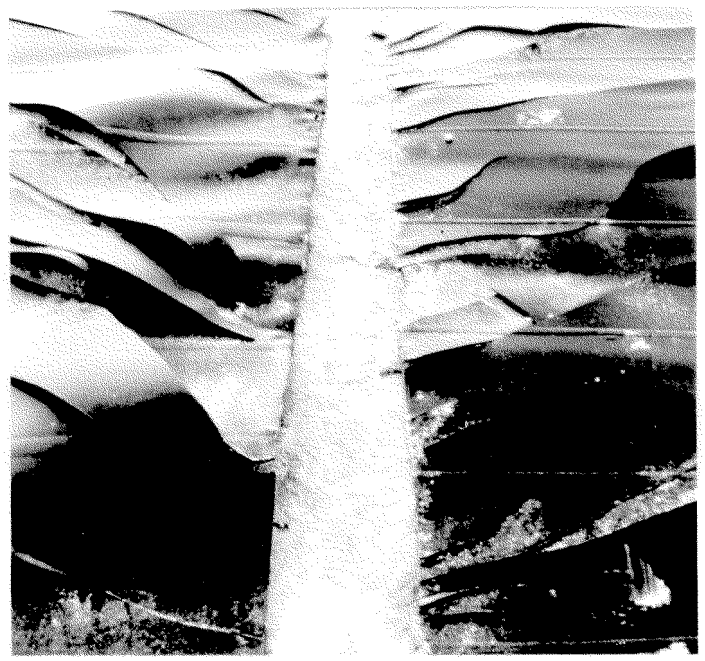

Fig. 23 Detail of central crack and shattering cracks branching from the central crack.

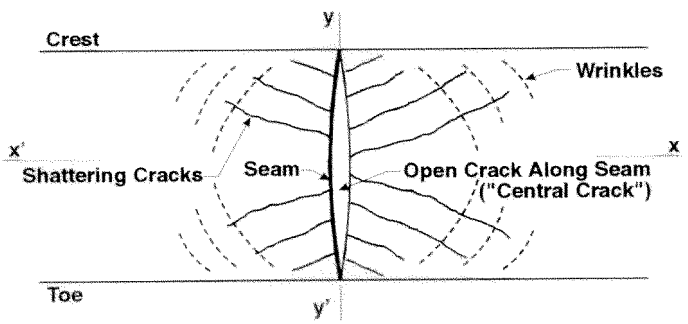

Fig. 24 Summary of observations.

crest and the toe of the slope seems consistent with a thermal contraction of the geomembrane in the direction parallel to the crest and the toe (since contraction in the direction of the slope is not possible because the geomembrane is fixed at the crest and the toe), but how is it possible that the same thermal contraction also create cracks that form an angle with the central crack and, furthermore, create wrinkles, which would indicate an expansion, not a contraction, of the geomembrane?

- Did the central crack occur first, then generating the shattering cracks and the wrinkles, or did all three phenomena occur simultaneously and/or independently?

It is important to answer these questions to understand the mechanism of shattering cracks and to help prevent the phenomenon: if it is shown that shattering cracks are a mere consequence of the development of the central crack, then all preventive efforts should focus on measures aimed at preventing the development of cracks along seams (a subject discussed in Section 5).

6.2 Summary of the Theoretical Analysis

A detailed theoretical analysis of the mechanism leading to quasi-symmetrical patterns of shattering cracks observed on the side slope of empty geomembrane-lined ponds has been published by Giroud (1994b). The analysis is based on the assumption that shattering cracks should occur in directions that are perpendicular to the directions of maximum stress and strain. Therefore, the analysis consists of evaluating the stresses and strains in the geomembrane before and after the opening of the central crack to determine if the opening of the central crack results in an increase in the maximum stress and strain and to determine the direction of the maximum stress and strain. The main steps of the analysis can be summarized as follows:

- The first step consists of evaluating the amount of geomembrane contraction due to the temperature decrease and other causes such as the irreversible shrinkage due to the release of stresses stored in the geomembrane at the manufacturing stage. It should be noted that the contraction thus evaluated does not occur prior to the opening of the central crack because the geomembrane is fixed at the crest and the toe of the slope and, therefore, cannot move. The constrained contraction results in a tensile stress in the geomembrane. It should also be noted that the constrained contraction and the resulting tensile stress do not necessarily have the same value in all directions. The anisotropy of tensile stress at this stage may be due to a difference in coefficient of thermal expansion between the roll and cross-roll directions of the geomembrane. Also, stresses stored in the geomembrane at the manufacturing stage are

usually different in the roll and cross-roll directions. At this stage (i.e., prior to the opening of the central crack) the principal directions of the stresses and strains are the geomembrane roll and cross-roll directions, i.e., the direction of the slope and the direction perpendicular to the slope.

- The second step consists of assuming that the crack along the seam opens as a result of the tensile stresses identified above. (The reasons why cracking occurs along a seam were discussed in Section 5.) Geometric considerations lead to a relationship between the opening of the central crack, $2\delta_o$, and the geomembrane contraction:

$$2\delta_o = d\ (\epsilon_{cx} + \nu\ \epsilon_{cy}) \qquad (13)$$

where: d = distance from the central crack beyond which the geomembrane does not move (and, consequently, cracking cannot develop); ϵ_{cx} = geomembrane contraction in the direction perpendicular to the central crack; and ϵ_{cy} = geomembrane contraction in the direction parallel to the central crack.

- The third step consists of analyzing the stresses and strains in the geomembrane after the opening of the central crack. As a result of the opening of the central crack, the geomembrane contracts in the direction perpendicular to the central crack (Figure 25). However, geomembrane contraction is not completely free since the geomembrane is fixed at the crest and the toe of the slope. This results in a distortion of the geomembrane, i.e., a rotation of the principal stresses and strains. The new direction and the magnitude of the principal stresses and strains are obtained using the Mohr's circles for stresses and strains, respectively.

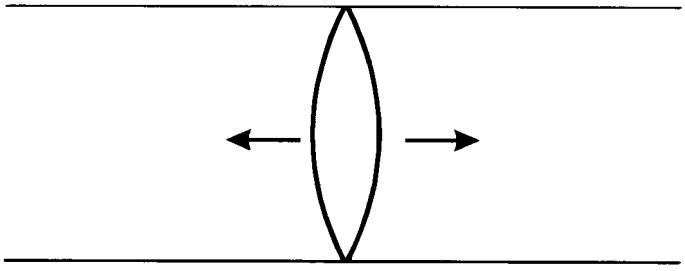

Fig. 25 Geomembrane contraction after opening of the central crack.

The main findings of the analysis can be summarized as follows:

- The directions of principal stresses and principal strains are the same. Therefore, assuming that cracks are perpendicular to the direction of maximum stresses is identical to assuming that they are perpendicular to the direction of maximum strains.
- The opening of the central crack causes an increase in the maximum strain everywhere in the geomembrane, except on the axis x′x and beyond the distance d from the central crack, which is consistent with the observations that show no shattering cracks on axis x′x and beyond a distance d from the central crack. The fact that the opening of the central crack causes an increase in the maximum strain in the geomembrane shows that geomembrane cracking can occur if, prior to the opening of the central crack, the geomembrane was close to the conditions that lead to cracking. This is possible if the geomembrane is made with a resin susceptible to cracking and is at low temperature, which reduces its strain at yield, as shown in Figure 9c.
- The maximum increase in the major principal strain occurs at the extremities of the central crack. This is illustrated in Figure 26, which shows that maximum distortion (which results in maximum strain increase) occurs at the extremities of the central crack. This is consistent with the greater density of shattering cracks in the vicinity of the extremities of the central crack shown in Figure 27.

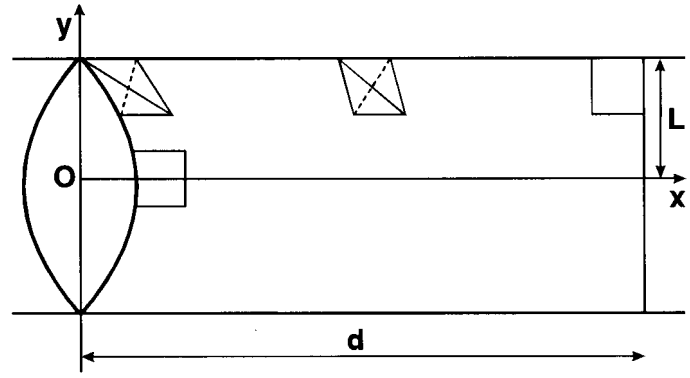

Fig. 26 Geomembrane distortion resulting from the opening of the central crack. (Notes: A rectangle without diagonals exhibits no distortion, a solid diagonal indicates expansion, and a dashed diagonal, contraction. The opening of the central crack is exaggerated.)

- The direction of principal strain varies from one point to another. Therefore the shattering cracks must have a curved shape. The orientation of the shattering cracks, derived from the principal strain direction, is expressed by the following equation:

$$\tan\theta = \sqrt{K^2 + 1} - K \qquad (14)$$

where θ is the angle between the axis Ox and the direction of shattering cracks. The value of K is

complex if the constrained contraction of the geomembrane that exists before the opening of the central crack is anisotropic. In the isotropic case, K is as follows:

$$K = \frac{1 - y^2/L^2}{(y/L)\ (d/L)\ (1 - x/d)} \qquad (15)$$

where: L = half-length of the central crack (i.e., half the distance between the crest and the toe of the slope); d = distance from the central crack beyond which the geomembrane does not move. The axes Ox and Oy are defined in Figure 26.

Using Equations 14 and 15 it is possible to establish the pattern of shattering cracks for any given value of the ratio d/L. (The reader is reminded that d, the distance from the central crack beyond which there are no shattering cracks, is related to the opening of the central crack through Equation 13.) The pattern of cracks in the case d/L = 2 is shown in Figure 27. Similar patterns for other values of d/L have been presented by Giroud (1994b).

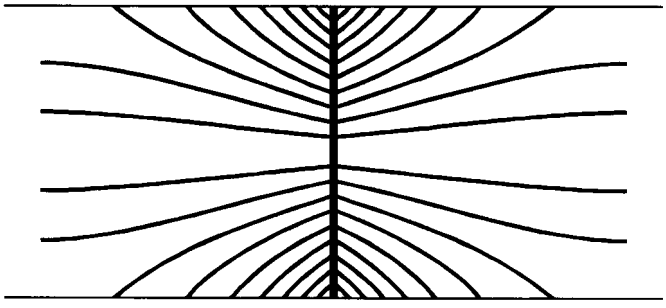

Fig. 27 Pattern of cracks for the case d/L = 2 (Giroud, 1994b).

The similarity between the theoretical pattern of cracks (Figure 27) and the observed pattern (Figures 22, 23 and 24) is noteworthy. The close agreement between the theoretical results and the observations establishes the validity of the initial assumption that the central crack opens first. Therefore, the theoretical study clearly establishes that the quasi-symmetrical shattering cracks are a consequence of the opening of the crack located along a seam.

As mentioned in Section 6.1, the shattered geomembrane exhibits wrinkles in directions approximately perpendicular to the shattering cracks. Giroud (1994b) has analyzed the evolution of stresses in the shattered geomembrane as the temperature increases from the very low temperature at the time of shattering to a higher temperature when observations are made, and demonstated that the observed wrinkles were not present at the time of shattering but result from the warming up of the geomembrane after shattering. Giroud also showed that the orientation of the wrinkles corresponds to the orientation of maximum compressive strain in the shattered geomembrane and that this orientation is approximately perpendicular to the orientation of the shattering cracks, which is consistent with the observations.

6.3 Discussion

The theory presented above should not be regarded only as an academic exercise. The in-depth understanding of the mechanical behavior of the geomembrane resulting from the rigorous analysis helps focus the attention on the fact that the geomembrane seam area is a delicate area where cracking may occur and cause shattering crack propagation into large areas of the geomembrane liner. Therefore, efforts should be made to minimize the risk of cracking along a seam, such as placement of the geomembrane with slack or compensation panels (i.e., large geomembrane undulations placed at regular intervals) to reduce tensile stresses in case of thermal contraction, seaming temperature control to avoid geomembrane overheating, and adequate grinding procedures (in cases where grinding is required prior to seaming). These recommendations remain valid, even though geomembranes that are less susceptible to stress cracking than the HDPE geomembranes used in the 1980s are becoming available.

Another practical result from the analysis is the recommendation by Giroud (1994b) that the maximum distance between compensation panels be equal to the length of the exposed slope (i.e., from crest to toe if the impoundment is empty). This recommendation results from a discussion of Equation 13.

Finally, the mere fact that the theoretical analysis provides a quantative description of the phenomenon that is consistent with observations illustrates that complex mechanisms associated with the behavior of geosynthetics can be rationally analyzed. This should encourage the development and publication of studies on the behavior of geosynthetics, which would benefit the geosynthetics discipline.

7 GEOMEMBRANE WRINKLES

7.1 Overview

Why do high density polyethylene (HDPE) geomembranes exhibit large wrinkles (Figure 28) when they are exposed to the sun? The well-known answer: because HDPE has a large coefficient of thermal expansion. This answer is misleading, although it is correct to state that HDPE has a large coefficient of

thermal expansion (i.e., about 10 times greater than the coefficient of thermal expansion of usual construction materials such as steel or concrete).

Polyvinyl Chloride (PVC) too has a high coefficient of thermal expansion (almost as high as that of HDPE); however, PVC geomembranes do not exhibit large wrinkles when they are exposed to the sun. Therefore, instead of accepting the traditional answer, it is preferable to conduct a rational analysis, which shows that the coefficient of thermal expansion is only one of the parameters that govern the formation of wrinkles.

Fig. 28 Typical HDPE geomembrane wrinkles.

7.2 Summary of the Theoretical Analysis

A detailed theoretical analysis of geomembrane wrinkles has been published by Giroud and Morel (1992). The principle of the analysis can be summarized as follows:

- As a result of the bending of the geomembrane that is associated with a wrinkle, there are two opposite forces, F, at the base of the wrinkle (Figure 29). The theoretical analysis shows that these forces are proportional to the elastic modulus of the geomembrane material and to the third power of the geomembrane thickness; the forces F are also a function (rather complex) of the size and shape of the wrinkle.
- The two forces F must be balanced by external forces, which are forces opposite to the forces F and applied to the wrinkle by the portions of the geomembrane located on each side of the wrinkle, i.e., the portions of the geomembrane in contact with the underlying soil. These external forces are the sum of shear stresses, τ, that result from the weight of the geomembrane and the interface friction between the geomembrane and the underlying soil (Figure 29). Therefore, they are proportional to the mass per unit area of the geomembrane, the distance between wrinkles and the geomembrane/soil interface friction coefficient.
- The size of the wrinkle (which has an influence on the magnitude of the forces F) is a function of the distance between adjacent wrinkles, the coefficient of thermal expansion of the geomembrane material, and the temperature difference to which the geomembrane has been subjected since the last time the geomembrane laid flat.

Fig. 29 Wrinkle equilibrium.

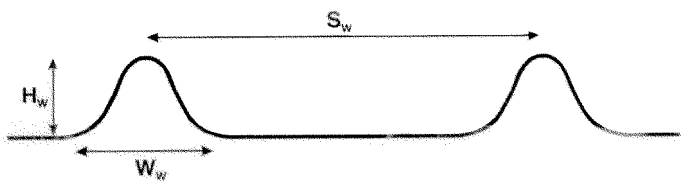

Fig. 30 Wrinkle geometry.

The analysis requires complex mathematical derivations involving elliptic integrals of the first and second kinds and leads to a series of equations that can only be solved numerically. The geometry of the wrinkles (defined by: H_w = wrinkle height, W_w = wrinkle width, and S_w = center-to-center spacing between adjacent wrinkles, as shown in Figure 30) is thus obtained as a function of the following parameters:

- the modulus of elasticity, E, thickness, t, and density, ρ, of the geomembrane;
- the geomembrane-soil interface friction angle, ϕ; and
- the geomembrane relative expansion, $\Delta L/L$, which is proportional to the temperature increase and the geomembrane coefficient of thermal expansion.

The analysis also gives the value of the maximum strain, which occurs at the top of the wrinkle, as a function of the shape and size of the wrinkle, i.e., as a function of the above parameters.

A parametric study shows that some approximations can be made, which allowed Giroud and Morel (1992) to establish the following approximate equations:

$$H_w \approx (\Delta L/L)\ S_w \tag{16}$$

$$S_w \approx \frac{1/2}{(\Delta L/L)^{2/3}} \left[\frac{E\ t^2}{\rho\ g\ \tan\phi}\right]^{1/3} \tag{17}$$

7.3 Discussion

Using the above equations, a parametric study has been conducted considering the following variables:

- Geomembrane type: HDPE and PVC, with elastic moduli, in the considered range of temperatures, of 250 MPa (HDPE) and 5 MPa (PVC).
- Geomembrane color: black or white, assuming on the basis of data provided by Pelte et al. (1994) that the maximum temperature reached in the field is 75°C for a black geomembrane and 50°C for a white geomembrane.
- Geomembrane roughness (for HDPE only): rough (textured) or smooth with an interface friction angle with the soil of 30° (rough) or 10° (smooth). (A friction angle of 20° was used for PVC geomembranes.)

All geomembranes were assumed to have been installed flat at a temperature of 20°C, and were assumed to have the same coefficient of thermal expansion, 1.5×10^{-4}/°C.

The results of the parametric study, rounded to allow for simple conclusions, are presented in Table 3.

Table 3. Wrinkle height and spacing as a function of geomembrane type, color and roughness.

Geomembrane Type and Roughness	Wrinkle Height	Wrinkle Spacing	
		Black	White
HDPE Smooth	60 mm	7.5 m	15 m
HDPE Rough	40 mm	5 m	10 m
PVC	10 mm	1 m	2 m

The following conclusions may be drawn from Table 3:

- The color of the geomembrane has very little influence on the height of the wrinkles (as a result of the rounding, no influence appears in Table 3), but has a marked influence on the spacing between wrinkles. Table 3 shows that there are approximately twice more wrinkles in a black geomembrane than in a white geomembrane.
- The wrinkle height and spacing in the case of a rough geomembrane are approximately two thirds of what they are in the case of a smooth geomembrane of the same type and color. In other words, for a given type and color of geomembrane, the total amount of wrinkling (i.e., the geomembrane thermal expansion) is the same, but the distribution of the wrinkles is different: if the geomembrane is rough the wrinkles are smaller and closer than if the geomembrane is smooth.
- PVC geomembranes have small wrinkles that are closely spaced. This is because the modulus of PVC geomembranes is very small compared to the modulus of HDPE geomembranes. As a result, the horizontal forces, F (Figure 29), are small in the case of PVC geomembranes, and only a short spacing between wrinkles is sufficient to mobilize geomembrane-soil interface friction to balance the force F.

From the above discussions, it appears that the most important factor that explains the observed difference in wrinkling between different types of geomembranes is not the coefficient of thermal expansion as usually mentioned, but the geomembrane modulus of elasticity. Therefore, when it is critical to minimize wrinkling, a geomembrane with a low modulus should be selected, if possible.

The study also shows that, for a given type of geomembrane polymer, the design engineer can decrease the geomembrane thermal expansion, hence the number (but not the height) of wrinkles by using geomembranes that are white on their face exposed to the sun, and can decrease the number and the height of wrinkles by using geomembranes that are rough (textured) on their face in contact with the underlying soil.

8 GEOSYNTHETIC RESISTANCE TO DIFFERENTIAL SETTLEMENT

8.1 Overview

Geosynthetics are often subjected to differential settlements and numerous failures have been observed, especially with geomembranes (Figure 31). It is generally considered that low-modulus geosynthetics (i.e., geosynthetics that stretch a lot under a given tension) are more likely to withstand differential settlements without damage than high-modulus geosynthetics. However, the geosynthetics response to differential settlement is complex and the solution is not as simple as often believed.

The geosynthetic response to differential settlement is a combination of stretching over, and displacement toward, the area where settlement occurs. A theoretical analysis of this mode of geosynthetic behavior is presented below.

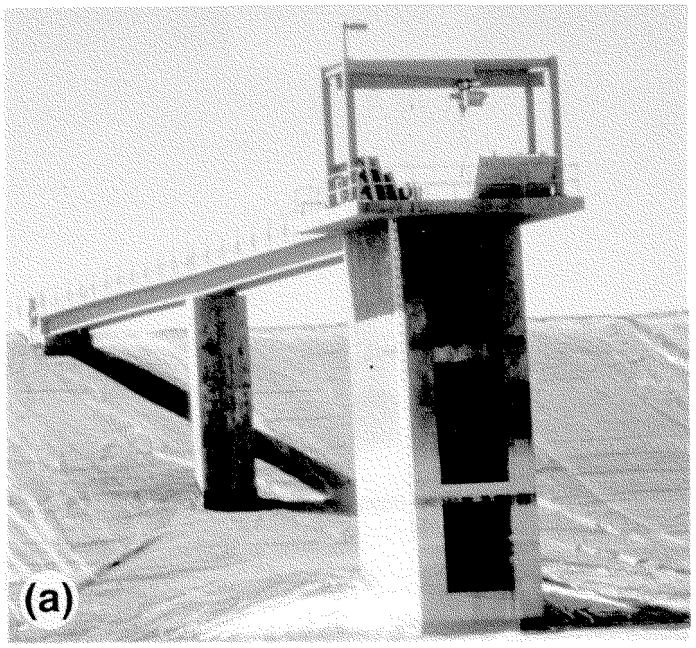

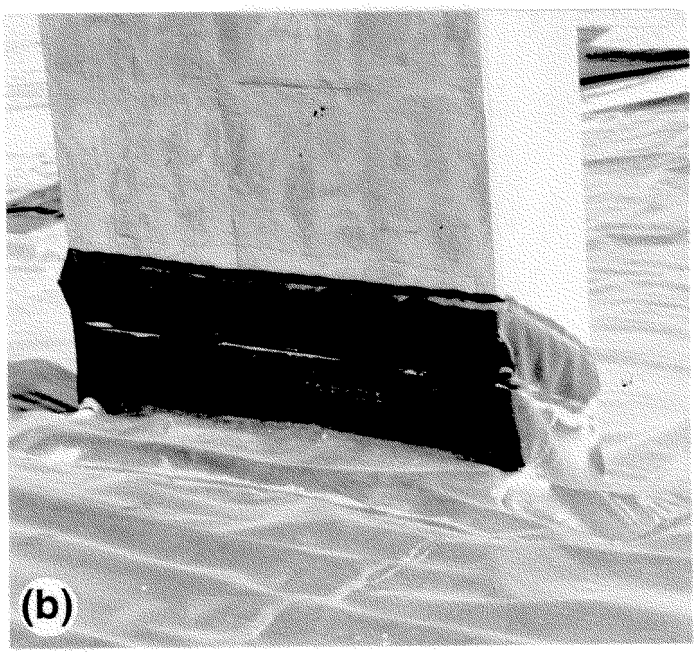

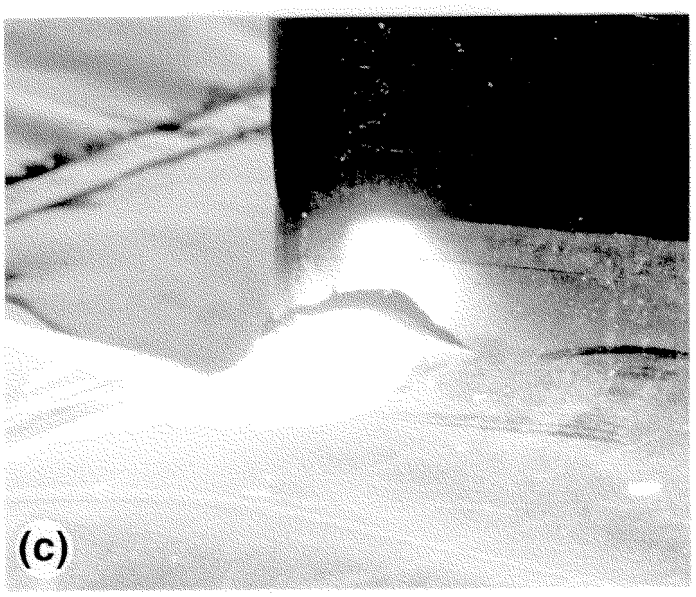

Fig. 31 Geomembrane connected to a concrete structure: (a) general view; (b) connection with the concrete structure; and (c) geomembrane failure at the corner of the concrete structure.

8.2 Summary of the Theoretical Analysis

The theoretical analysis is presented in the case of a geomembrane subjected to a differential settlement between a concrete structure and an earth dike. However, the results of the analysis are applicable to all cases of differential settlement and all geosynthetics.

The situation of the geomembrane, resting on an earth dike and connected to a concrete structure, is defined in Figure 32a. The pressure on the geomembrane is assumed to be uniformly distributed and, consequently, the interface shear stresses between the geomembrane and the supporting soil are uniformly distributed (Figure 32b). As a result, the tension in the geomembrane, which is balanced by the interface shear stresses, is linearly distributed (regardless of the characteristics of the geomembrane) (Figure 32c). Therefore:

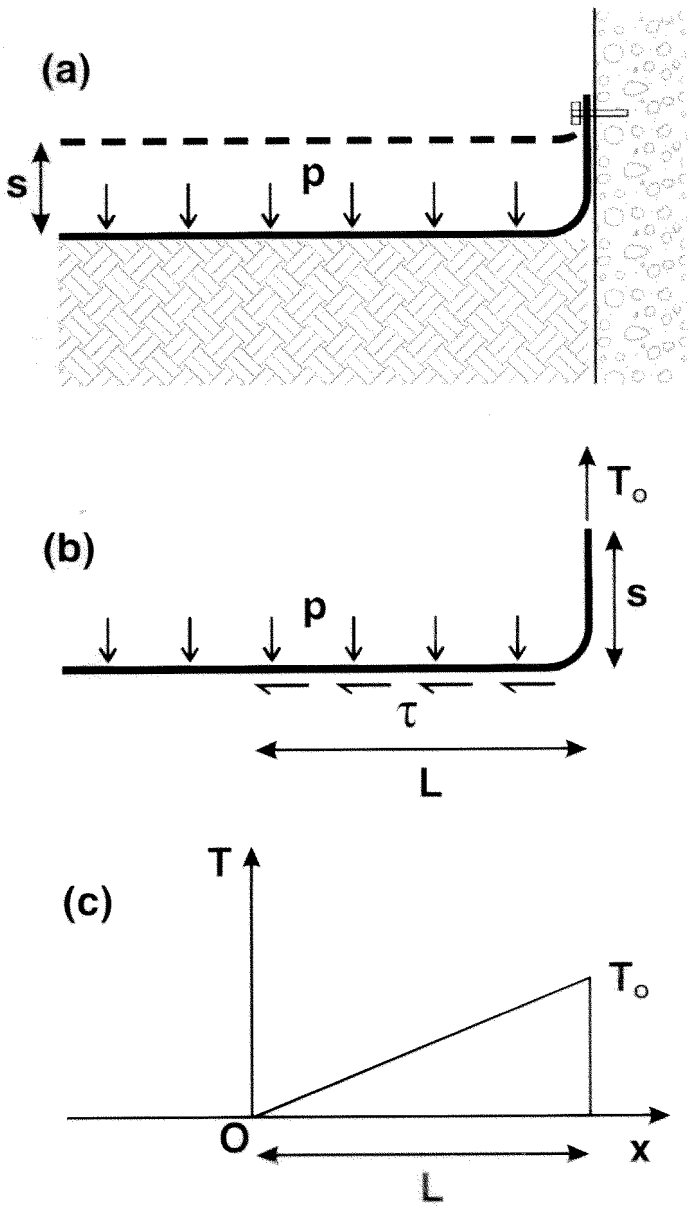

Fig. 32 Geomembrane subjected to differential settlement, s: (a) geomembrane before and after settlement; (b) tension and stresses; and (c) geomembrane tension distribution.

$$T = \tau x \quad (18)$$

where: T = geomembrane tension at abscissa x; and τ = interface shear stress defined by:

$$\tau = p \tan\phi \quad (19)$$

The maximum tension in the geomembrane is:

$$T_o = \tau L \quad (20)$$

where: L = length over which the geomembrane stretches and the interface shear stresses are mobilized.

Both T_o and L are unknown and they can be determined as follows. The total elongation of the geomembrane must be equal to the settlement, s. This elongation is obtained, as follows, by integrating the geomembrane strain, ϵ, over the length L:

$$s = \int_0^L \epsilon \, dx \quad (21)$$

Combining Equations 18 to 21 gives:

$$s \, p \tan\phi = \int_0^{T_o} \epsilon \, dT \quad (22)$$

This integral is equal to the area between the geomembrane tension-strain curve and the tension axis (OT) up to the level $T = T_o$ (Figure 33). This leads to the proposed definition of a new concept: the co-energy associated with the geomembrane tension-strain curve (Figure 34). The terminology co-energy is proposed since the area between the geomembrane tension-strain curve and the strain axis ($O\epsilon$) is known to be the energy associated with the geomembrane tension-strain curve.

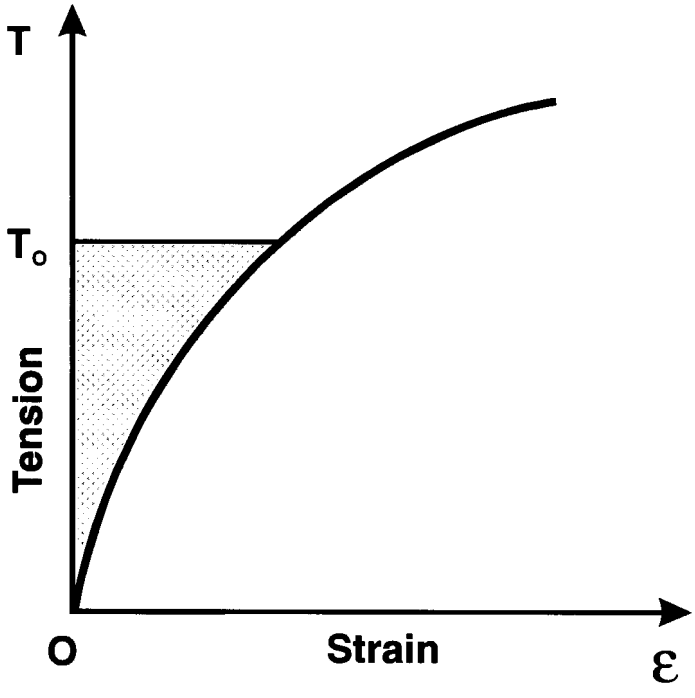

Fig. 33 Geomembrane tension-strain curve and area defining the geomembrane co-energy up to the level $T = T_o$.

Knowing the tension-strain curve of the considered geomembrane, it is possible to determine the co-energy, E′, either analytically in rare cases where the equation of the geomembrane tension-strain curve is known, or, at least, numerically. Then the following equation, derived from Equation 22, may be used:

$$s_{max} \, p \tan\phi = E' \quad (23)$$

hence:

$$s_{max} = \frac{E'}{p \tan\phi} \quad (24)$$

This equation gives the value of the maximum differential settlement, s_{max}, that the geomembrane can withstand if the applied pressure is p and the interface friction angle is ϕ.

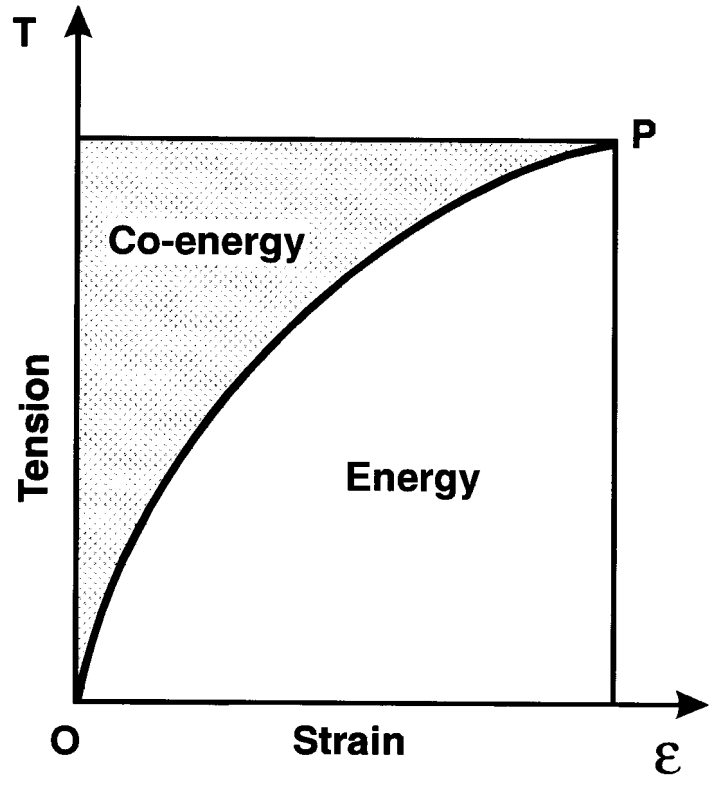

Fig. 34 Energy and co-energy associated with a tension-strain curve. (Note: P is the peak of the tension-strain curve, whether it is a yield peak or the maximum of the curve at, or close to, break.)

The co-energy concept appears to be a powerful tool that ranks geomembranes according to their ability to withstand differential settlements. For example, geomembrane (2) (Figure 35) has a greater co-energy than geomembrane (1) and, therefore, can tolerate larger differential settlements. It should not however be concluded that the geomembrane with the larger strain at the peak of its tension-strain curve can always tolerate the larger differential settlements. As shown in Figure 36, a geomembrane with a smaller strain at the peak

may have a greater co-energy and may, therefore, tolerate larger differential settlements. Clearly, the criterion is the co-energy, not the strain at the peak of the tension-strain curve.

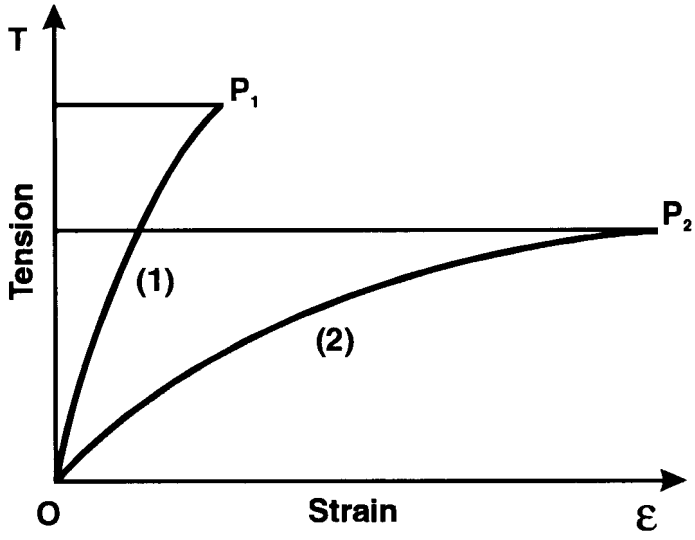

Fig. 35 Comparison of two geomembranes.

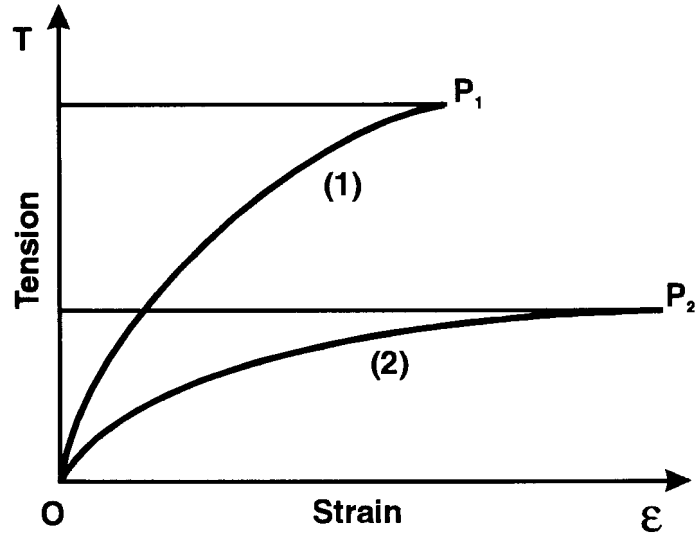

Fig. 36 Comparison of two geomembranes.

The co-energy concept can also be used to compare candidate geomembranes for a given differential settlement problem. The applied pressure, p, and the differential settlement, s, are the same for all candidate geomembranes, but the interface friction angles and the tension-strain curves are different. The value of the required co-energy is calculated as follows for each of the candidate geomembranes:

$$E'_{reqi} = s\ p\ \tan\phi_i \qquad (25)$$

The factor of safety for each candidate geomembrane regarding differential settlement may then be calculated as follows:

$$FS_i = \frac{E'_i}{E'_{reqi}} \qquad (26)$$

where E'_i is the co-energy associated with the geomembrane tension-strain curve (i.e., the total area between the tension-strain curve and the OT axis as shown in Figure 34) and E'_{reqi} is the required co-energy.

Two geomembranes may have the same tension-strain curve, but different interface friction angles with the supporting soil, one geomembrane being smooth, the other textured. Having the same tension-strain curve, these two geomembranes have the same co-energy, but, according to Equation 25, the required co-energy is greater for the textured geomembrane because the friction angle is greater. As a result, the textured geomembrane has a lower factor of safety regarding differential settlements. This potential problem with textured geomembranes should be taken into account in design.

8.3 Discussion

A rigorous analysis of the mechanism of deformation of a geomembrane subjected to differential settlement shows that the ability of a geomembrane to withstand differential settlements is not, as often mentioned, characterized by a low modulus or a large strain at yield or break. The analysis shows that the proper way to evaluate the geomembrane ability to withstand differential settlements is through the co-energy, a new concept proposed by the author.

The concept of co-energy has been introduced using the example of a geomembrane subjected to a differential settlement at its connection with a rigid structure. However, the concept can be used for all geosynthetics in all cases of differential settlement.

CONCLUSIONS

On the basis of several examples, this paper shows that the behavior of geosynthetics can be quantified using rational analyses and that design engineers should be careful when they use methods imported from other disciplines, such as geotechnical engineering. Also, design engineers should be particularly circumspect with methods justified by common sense, because common sense is generally a screen put forward to hide the laziness inspired by the difficulty inherent to rational analyses.

The mere fact that theoretical analyses provide quantative descriptions of phenomena which are consistent with observations illustrates that complex

mechanisms associated with the behavior of geosynthetics can be rationally analyzed. This should encourage engineers to rationally design geosynthetic applications instead of using empirical approaches. This should also encourage the development and publication of studies on the behavior of geosynthetics, which would benefit the geosynthetics discipline.

This paper is essentially illustrated with examples of design methods and concepts developed by the author. This should not be construed as meaning in any way that there are no other methods for quantifying the behavior of geosynthetics. However, in order to be able to dissect the selected examples, the author had to be intimately familiar with the mechanisms and theories involved.

The methods used to analyze the examples presented in this paper are methods that stem from fundamental mechanics and mechanics of continua. This is because the author is familiar with these methods and has used them extensively. It is acknowledged however that polymer science provides another source of fruitful methods which can be used to understand and quantify the behavior of geosynthetics. A similar paper written by a polymer scientist would be most welcome, and even better would be a paper on the same subject co-authored by a geotechnical engineer and a polymer scientist.

The section of this paper on geomembrane stress cracking shows that a purely mechanical approach can shed some light on a problem that has traditionally been considered a specialty of polymer scientists. There is no private domain. Polymer scientists should write about "geotechnical" subjects such as filtration. Engineers designing geotextile filters would certainly learn a lot from such a paper, just like many geotechnical engineers would learn about sand filters reading some sections of the paper presented herein, although it was written with geosynthetics in mind.

Finally, on a more personal note, the author recognizes that the opportunity to present this special lecture is an exceptional honor, and expresses his gratitude to the organizers of the 5th International Conference on Geotextiles, Geomembranes and Related Products, to the International Geotextile Society, and to all colleagues who have encouraged his work over the years The author hopes that the work presented herein will serve the geosynthetics discipline.

ACKNOWLEDGMENTS

The author is grateful to K.L. Soderman for his review and valuable comments, and to T. Pelte, G. Saunders and S. Berdy for their assistance in the preparation of this paper.

REFERENCES

Giroud, J.P. (1978), "*Unpublished Notes on a Mathematical Model of Geotextile Filter Clogging*".

Giroud, J.P. (1982), "Filter Criteria for Geotextiles", *Proceedings of the Second International Conference on Geotextiles*, Vol. 1, Las Vegas, NV, USA, 1: 103-108.

Giroud, J.P. (1984a), "Analysis of Stresses and Elongations in Geomembranes", *Proceedings of the International Conference on Geomembranes*, Denver, CO, USA, 2: 481-486.

Giroud, J.P. (1984b), "*Geotextiles and Geomembranes. Definitions, Properties and Design*", IFAI Publishers, 325 p.

Giroud, J.P. (1988), "Review of Geotextile Filter Criteria", *Proceedings of the First Indian Geotextiles Conference*, Bombay, India, :1-6.

Giroud, J.P., and Morel, N. (1992), "Analysis of Geomembrane Wrinkles", *Geotextiles and Geomembranes*, 11, 3: 255-276.

Giroud, J.P. (1993), "Lessons Learned from Studying the Performance of Geosynthetics", *Proceedings of Geotextiles-Geomembranes Rencontres 93*, Joué-les-Tours, France, 1: 15, 33-46.

Giroud, J.P., Soderman, K.L., and Monroe, M. (1993), "Mechanical Design of Geomembrane Applications", *Proceedings of Geosynthetics '93*, Vancouver, Canada, 3: 1455-1468.

Giroud, J.P. (1994a), "Mathematical Model for Geomembrane Stress-Strain Curve with a Yield Peak", *Geotextiles and Geomembranes*, 13, 1: 1-22.

Giroud, J.P. (1994b), "Determination of Geomembrane Shattering Cracks", *Geosynthetics International*, 1, 2: __-__.

Giroud, J.P., Monroe, M., and Charron, R.M. (1994a), "Measurement of HDPE Geomembrane Strain in Tensile Test", *Geotechnical Testing Journal*, ASTM, 17, 1: 65-71.

Giroud, J.P., Beech, J.F., and Soderman, K.L. (1994b), "Yield of Scratched Geomembranes", *Geotextiles and Geomembranes*, 13, 4: 231-246.

Giroud, J.P., Tisseau, B., Soderman, K.L., and Beech, J.F. (1995), "Analysis of Strain Concentrations Next to Geomembrane Seams", to be published.

Pelte, T., Pierson, P. and Gourc, J.P. (1994), "Thermal Analysis of Geomembranes Exposed to Solar Radiation", *Geosynthetics International*, 1, 1: 21-44.

Soderman, K.L. and Giroud, J.P. (1994), "Relationships Between Uniaxial and Biaxial Stresses and Strains in Geosynthetics", submitted to *Geosynthetics International*.